# Brecciation among 2280 ordinary chondrites - constraints on the evolution of their parent bodies

**Addi Bischoff[1], Maximilian Schleiting[1,2], Rainer Wieler[3], and Markus Patzek[1]**

**[1]Institut für Planetologie, Westfälische Wilhelms-Universität Münster, Wilhelm-Klemm-Str. 10, D-48149 Münster, Germany**

**[2]Institut für konstruktiven Ingenieurbau, Universität Kassel, Mönchebergstr. 7, D-34125 Kassel, Germany**

**[3]ETH Zürich, Departement Erdwissenschaften, Clausiusstr. 25, CH-8092 Zürich, Switzerland.**

**Corresponding author: Addi Bischoff**

**Email: bischoa@uni-muenster.de**

**Geochimica et Cosmochimica Acta**

**Revised version, June 18, 2018**

## Abstract

After accretion of meteorite parent bodies, larger and smaller collisions have led to significant modifications of these bodies. Involved processes include excavation of material, thermal metamorphism, melting, mixing of different materials, re-accretion, and re-lithification. All these processes can be repeated several times. In this study polished thin sections (PTS) of 2280 chondrites (1193 H, 947 L, and 140 LL chondrites) were investigated in order to obtain the abundance of brecciated rocks among the ordinary chondrites. In addition, we have determined the abundance and characteristics of shock vein-bearing H, L, and LL chondrites and of impact melt rock clasts. We also recognized xenolithic components based on O-isotope studies. Noble gas data were considered in order to detect regolith breccias and to discuss late impact histories. The investigation of 2280 samples shows that 23% (276 of 1193) of the H chondrites, 23% (220 of 947) of the L chondrites, and 79 % (110 of 140) of the LL chondrites are brecciated. Considering the heavily-brecciated LL chondrites in 63 of the 140 chondrites (45%) shock veins were clearly detected. 57 of these 63 chondrites are brecciated rocks. The investigation of the H and L chondrites has shown that about 26% (310 of 1193) of the H chondrites and 40% (379 of 947) of the L chondrites contain shock veins. In our data-set 20% of the H chondrites and 8.3% of the LL chondrites, but only 3.0% of the L chondrites contain solar noble gases. Remarkably, about 62% of all brecciated H chondrites (with noble gases analyzed) contain solar noble gases compared to only around 11% and 10% of the brecciated L and LL chondrites, respectively. The identification of xenolithic clasts (e.g., CI-, CM-, and ureilite-like lithologies) in primitive type 3 chondrites indicates simultaneous accretion of clasts and chondrules. These clasts must have been formed early within the first 2 Ma on subsequently-destroyed precursor, first generation parent bodies. The formation of complex breccias witnesses the collisions between asteroids of very different lithologies and heritage. Although the onion-shell configuration of primordial parent bodies is necessary in order to form the chondrites with different degrees of metamorphic overprint (petrologic types 3-6) subsequent catastrophic fragmentation and reassembly to form asteroids with a rubble-pile structure are required to explain certain features discussed in this work. However, distinct peaks in the cosmic ray exposure age distributions indicate that not too many impacts in the last 100 Ma were responsible to deliver the majority of the ordinary chondritic meteoroids to Earth. Yet, this certainly does not tell anything about the number of “last-generation” parent bodies that exist in the asteroid belt, since S-type asteroids are the most abundant type of asteroid in the inner main belt and thought to be the parent bodies of ordinary chondrites.

## 1. INTRODUCTION

Brecciated meteorites provide unique information about the history of asteroids and impacts on small bodies in our solar system and represent samples from a variety of parent bodies (e.g., Keil, 1982; Stöffler et al., 1988; Bischoff et al., 2006).

Due to collisions between large asteroids as well as less catastrophic impacts, different processes lead to the modification of meteorite parent bodies, the formation of new bodies, and new rock types. These processes include, e.g., accretion, excavation of material, thermal metamorphism, melting, mixing of different materials, re-accretion, and re-lithification (e.g., Bischoff and Stöffler, 1992; Bischoff et al., 2006). All these processes can be repeated multiple times and may lead to meteorite breccias that contain a large variety of fragments and lithologies. Details on impact and cratering processes including the physical and mineralogical aspects are described in detail by Stöffler et al. (1988, 2018). Brecciation is a very important and characteristic process affecting meteorites; thus, many known meteorites are brecciated. High abundances of breccias occur among the carbonaceous chondrites (e.g., all CI and CM chondrites), mesosiderites, aubrites, and the HED meteorites (e.g., Bischoff et al., 2006). Also, ordinary chondrites are shocked to various degree (Stöffler et al., 1991) and are often heavily brecciated (e.g., Binns, 1967; Keil, 1982; Scott et al., 1989; Stöffler et al., 1988; Bischoff et al., 1993a, 2006). In 1967, Binns (1967) studied 361 ordinary chondrites and identified ~66% LL chondrites as breccias as well as ~33% and ~20% as H and L chondrite breccias, respectively. Scott et al. (1989) published similar data concerning the abundances of breccias (H: 24%; L: 18%; LL: 58%).

Furthermore, some fragments in polymict breccias represent xenolithic lithologies. In the past many foreign clasts within achondritic and chondritic breccias were often described as dark "carbonaceous" inclusions, but true CI- or CM-like clasts are rare (e.g., Zolensky et al., 1992, 1996; Bischoff et al., 1993b,c; Mittlefehldt, 1994; Endress et al., 1994; Rubin and Bottle, 2009; Funk et al., 2011; Patzek and Bischoff, 2015; Patzek et al., 2016, 2017, 2018). These and other foreign fragments may originate from unknown parent bodies or unknown lithologies from sampled parent bodies (e.g., Keil, 1982; Zolensky et al., 1992, 1996; Bischoff et al. 1993a, 2006; Horstmann and Bischoff, 2014). In this respect exceptional breccias are Kaidun (e.g., Zolensky et al., 1992; Zolensky and Ivanov, 2003) and Almahata Sitta (e.g., Bischoff et al., 2010; Goodrich et al., 2014; Horstmann and Bischoff, 2014), which both contain fragments of several different meteorite groups and classes. Kaidun consists of mm to sub-mm sized fragments of EH3-5, EL3, CV3, CM1-2, CI, and R chondrite fragments, which are mixed with numerous other unique lithologies (Ivanov, 1989;

Zolensky and Ivanov, 2003). The Almahata Sitta breccia contains different lithologies of ureilitic as well as other achondritic and chondritic lithologies including most petrologic types of EL and EH chondrites, and, additionally, H, L, LL, R, and C chondritic lithologies (e.g., Bischoff et al., 2010, 2012, 2014, 2015, 2016; Horstmann et al., 2010; Zolensky et al., 2010; Horstmann and Bischoff, 2014; Fioretti et al., 2017).

The aim of this study is to reveal information about the abundance of brecciated meteorites and their significance among the H, L, and LL ordinary chondrites. We have studied thin sections of 2280 chondrites. Preliminary results were published by Schleiting (2014, 2017) and Schleiting and Bischoff (2015, 2017) and details on some individual breccias were earlier studied by and with members of our group (e.g., Bischoff et al. 1993a, 2013a,b, 2017; Semenenko et al., 2001; Niemeier and Bischoff, 2006; Sokol et al., 2007a; Metzler et al., 2011; Funk et al., 2011; Dyl et al., 2012; Trigo-Rodriguez et al., 2014; Morlok et al., 2017). We also use published noble gas data available for ~12% of the meteorites studied here to recognize regolith breccias and to evaluate similarities and possible differences in cosmic-ray exposure age distributions between brecciated and non-brecciated meteorites.

## 2. SAMPLES, ANALYTICAL TECHNIQUES, AND BRECCIA DEFINITION

### 2.1. Samples

In this study, polished thin sections (PTS) of 1193 H, 947 L, and 140 LL chondrites were investigated in order to obtain the abundance of brecciated rocks among these chondrites (Table 1). A list of all samples studied with some further information is given in Table A1 of the Supplements and the appropriate explanations and notations of the Table are given in Chapter 2.2. All samples were available at the Institut für Planetologie (Münster) and the thin section size is given in Table A1. The thin section size can be very important as discussed in Chapter 2.4. Schleiting and Bischoff (2017) published preliminary results on the brecciation features found in PTS and hand-specimen. Since details on the brecciation of the hand-specimen were difficult to obtain in many cases, the discussed results of this work are solely based on the study of the polished thin sections, with some exceptions where the presence of solar-wind implanted noble gases indicates a regolith breccia. This was the case for the H chondrites Acfer 006, Acfer 095, Dimmitt, Fleming, Plainview, Pultusk, Tell, Gladstone, and the LL chondrite St. Mesmin. In addition, some meteorites that are listed as breccias in the MetBull database could not be identified as breccias in our thin sections. However, these meteorites were adopted as breccias in this study.

## 2.2. Explanations for Table A1 of the Electronic Supplement

After the first column with the "Name" of the chondrite the second column shows the thin section number of the Institut für Planetologie (PL = Planetologie; like PL93116).

The "Classification" of the chondrite is followed in the next column. This needs some explanations. Among the chondrites the chondrule size increases from H to LL chondrites and the metal abundance decreases in the same order. In some cases the database of the Meteoritical Bulletin lists chondrites like L(LL)3 or L/LL5. In these unclear cases of classification we have assigned the samples to a distinct class based on our estimate about the chondrule size and/or the abundance of metal. As an example, an L/LL5 sample can be either found in the list of the L5 or LL5 chondrites. Brecciated meteorites are indicated by a "√".

The "√" in the following column "Sh.V." indicates the presence of shock veins in the sample. Under "Sh.V. Location" it is noted - if the shock veins cut through the whole meteorite (W.m.) or if they are restricted to individual fragments within a chondrite breccia. The determined shock degree "Sh.D" after Stöffler et al. (1991) is followed in the next column.

The column "Noble /solar gases" indicates all meteorites with available noble gases (first "√" and with (second "√") or without (-) trapped solar noble gases. The column "T-exp" lists cosmic-ray exposure ages (in Ma), based on cosmogenic noble gas data. The majority of these ages (printed in normal font) are from the He-Ne-Ar age compilations by Marti and Graf (1992) and Graf and Marti (1994, 1995). Some ages (given in italics) are based on more recent Ne analyses and calculated according to Dalcher et al., 2013), whereby a shielding correction was applied if the ratio $(^{22}Ne/^{21}Ne)cos$ was $\geq 1.08$ and an "average" shielding (corresponding to $(^{22}Ne/^{21}Ne)cos = 1.11$) was adopted otherwise.

In the last column the size of the studied polished thin section is indicated ("PTS-size"). The size is given in $cm^2$.

Data on noble gases were taken from the compilation of Schultz and Franke (2004, and references therein) except for those of the meteorites Kosice (H5), NWA 869 (L3-6), and Vicencia (LL3.2) (Povinec et al., 2015; Welten et al., 2011; Keil et al., 2015).

## 2.3. Analytical Techniques

The investigation of the PTS regarding the abundance of breccias and the shock vein-bearing chondrites was carried out with the optical light microscope (*Zeiss Axiophot*) at the Institut für Planetologie of the Westfälische Wilhelms-Universität (WWU) Münster. Images in transmitted (plane and crossed polarizers) and reflected light were taken with an integrated *Olympus XC30*-camera. For the documentation of the results the software *analySIS pro* by *Olympus* was used.
Imaging and characterization of shock veins were partly done with a JEOL 6610LV scanning electron microscope (SEM) at the Interdisciplinary Center for Electron Microscopy and Microanalysis (ICEM, Münster). Images were taken mainly using backscattered electrons (BSE); the attached EDX (Energy dispersive X-ray spectroscopy) system (INCA by *Oxford Instruments*) was used for mineral identification.

The oxygen isotopic composition of olivine and pyroxene grains within three xenolithic clasts from the ordinary chondrite breccias Sahara 98645 (H3), Adrar 003 ((LL3.10), and NWA 5697 (L3) were obtained using the IMS1280-HR ion probe at the University of Heidelberg (Table 2). $^{16}O$, $^{17}O$, and $^{18}O$ were analyzed by utilizing a 10 keV $Cs^+$ primary ion beam with a beam current of 4-5 nA sputtering an analyses area of 6x6 µm (20x4s). Pre-sputtering of 8x8 µm before each analysis was carried out to increase secondary ion yields. Negative ions were collected by Faraday cups and corrected for IMF by analyzing in-house San Carlos olivine and pyroxene grains, which have been pre-measured by laser fluorination mass spectrometry at the University of Göttingen. Baselines were determined separately with 400s integration time. MRP was set to ~7000 for $^{17}O$ and ~2500 for $^{16}O$ and $^{18}O$. Charge compensation was accomplished by using the NEG.

Results are reported in δ-notation versus VSMOW with typical precision of ±0.3 ‰ in $\delta^{18}O$ and ±0.5 ‰ in $\delta^{17}O$.

### 2.4. Definition of different breccias and impact melt fragments in this work

Breccias are rocks that contains clasts of one or different petrographic type(s), and/or may contain fragments of xenolithic rocks, or impact melt fragments. Rocks containing solar wind implanted noble gases are defined as “regolith breccias”. For the classification of brecciated ordinary chondrites, the petrologic types of the meteorites and their fragments were determined. The classification of brecciated meteorites is defined by the least equilibrated fragment within the meteorite. For example, if a chondrite breccia contains fragments of the petrologic types 3, 4 and 5, the bulk breccia is defined as a type 3-5 breccia (genomict-polymict). In this respect, the rock is

polymict based on the coexistence of clasts representing three different lithologies, but genomict because the clasts belong to the same compositional chondrite group (e.g., Wasson, 1974; Bischoff et al., 2006). If a meteorite contains fragments of petrologic types 5 and 6 it is declared as type 5-6 breccia (genomict-dimict). Consequently, brecciated type 6 chondrites are always monomict breccias, as the occurrence of fragments with a lower petrologic type would change the classification of the meteorite breccia. A type 3 chondrite mentioned in the following study is not only a monomict type 3 rock, but also includes the breccia types X3-4, X3-5, and X3-6 (X = H, L, or LL). The abundance of various types of rock in the breccia is insignificant.

Microscopic studies reveal that type 3 and type 4 H-group ordinary chondrites contain many more mineral and chondrule fragments as L and LL chondrites of similar petrologic type. However, a clear brecciated texture was difficult to attest for these H-chondrites of low petrologic types. Another difficulty for identifying breccias of ordinary chondrites is related to the appearance of weathered rocks (especially of H-chondrites). Based on the high metal content of fresh H chondrites weathering leads to inhomogeneous formation of rust and other alteration products within the meteorite finds. This can lead to the impression in having a brecciated rock with fragments of different brownish taints. We tried to handle this issue very conservatively and classified only those ordinary chondrites as breccias, in cases where individual clasts were clearly visible.

Impact melt breccias are defined as shock-melted rocks with unmolten clasts. Chondrites that contain single impact melt fragments are not classified as impact melt breccias, but as breccias containing impact melt clasts (Table 3). Usually, impact melts have an igneous texture and consist of euhedral to subhedral olivine and pyroxene grains and clasts of the target rock embedded into a fine-grained (or glassy) mesostasis. Minerals are often zoned indicating fast cooling. Another characteristic feature of impact melts is the existence of droplets of immiscible sulfide and Fe-Ni metal, which are not observed in chondrules. Based on these features impact melt clasts cannot be fragments of macrochondrules, which typically have radial, barred, or cryptocrystalline textures and no metal-sulfide intergrowths (Weyrauch and Bischoff, 2012).

Considering the possibilities of positive recognition of shock vein-bearing or brecciated chondrites the critical aspects to consider are (a) the sample size and (b) the sample location in a rock. This can be excellently demonstrated by comparison of the rock features in different thin sections of Tenham (L6; Fig. 1). In the first sample shock veins are barely visible and if the sample size would be reduced to a thin section with a ~1 cm rock sample such an area may not even contain a single thin shock vein (Fig. 1a). In Fig. 1b the situation is certainly different and thick shock veins are clearly

visible. In a different area the monomict brecciation of Tenham is very obvious (Fig. 1c). In our study Tenham has been classified as a monomict L6 breccia, but as shown by the images of Fig. 1 very different classifications could be possible considering different sample sizes and locations varying from a “rock without shock veins”, over “shock vein-bearing chondrite” to “chondritic breccia”. A very similar situation may arise, if several individuals from a meteorite strewn field are classified. A good example is the complex LL5-6 breccia Chelyabinsk (e.g., Bischoff et al., 2013b; Morlok et al., 2017). Depending on the characteristics of the main lithologies of the rocks the meteorite can be classified as (a) a shock-veined LL chondrite, (b) a complex breccia, (c) a shock-darkened LL chondrite or (d) an impact melt breccia (Fig. 2).

Regolith breccias could only be recognized as such in the few cases where the presence of solar wind implanted noble gases unequivocally indicates that at least some grains of the meteorite had at least once been at the immediate surface of its parent body regolith. We mostly rely on the noble gas data compilation by Schultz and Franke (2004) augmented by a few more recent updates (see Table A1). Criteria to recognize solar noble gases are the Ne isotopic composition as well as elemental ratios $^{4}He/^{20}Ne$ and $^{20}Ne/^{36}Ar$ of trapped noble gases. In many cases only a fraction of the published analyses indicates a solar contribution, since samples from the interior of a larger regolithic pebble will be devoid of implanted solar wind atoms (e. g., Wieler et al., 1989a,b). We may thus have missed some regolith breccias even among the meteorites for which noble gas data are available.

## 3. RESULTS

The results of the study include observations and details on (1) the abundance of brecciated H, L, and LL chondrites, (2) the abundance and characteristics of shock vein-bearing H, L, and LL chondrites, (3) the abundance and characterization of impact melt rock clasts and (4) the recognition of xenolithic components based on O-isotope studies (see Table A1 in the Supplements).

### 3.1. Abundance of brecciated H, L, and LL chondrites

The investigated thin sections of 2280 chondrites revealed that 23% (276 of 1193) of the H chondrites, 23% (220 of 947) of the L chondrites and 79 % (110 of 140) of the LL chondrites are brecciated (Tables 1, 4, and A1; Fig. 3).

High abundances of brecciated LL chondrites were registered for all petrologic types (71-90%). Considering the H and L chondrites, rocks having components (fragments) of low petrologic types (types 3 and 4 chondrite) are often breccias. Many of these also have highly equilibrated clasts (e.g., H3-6 or L3-5 etc.). In detailed numbers, about 67% of the H chondrites and ~70% of the L chondrites having unequilibrated type 3 components are brecciated. Considering the petrologic type 4 chondrites (H(or L)4, H(or L)4-5, H(or L)4-6) 21% of the H chondrites and 33% of the L chondrites are brecciated. In H and L chondrites with petrologic type 5 (H(or L)5, H(or L)5-6) about 17% and 22%, respectively, of the meteorites are brecciated. H and L chondrites with petrologic type 6 (H6, L6) contain about 18% and 15% breccias, respectively. A decreasing abundance of breccias with increasing petrologic type of the meteorites is recognizable. This important finding will be discussed in detail below. Overall, the differences in the abundance of brecciated meteorites regarding the petrologic type between H and L chondrites are relatively small. Some examples of different breccias are given in Fig. 4.

### 3.2. Chondritic and achondritic fragments in brecciated ordinary chondrites and their O-isotope compositions

Some type 3 ordinary chondrites contain highly-primitive and equilibrated components as defined by the composition of FeO-bearing olivine (Grossman and Brearley, 2005). Most or perhaps all of these chondrites are breccias and were earlier defined as accretionary breccias (Kracher et al., 1982; Scott and Taylor, 1982; compare the review on breccias in Bischoff et al. (2006)). Some breccias (sometimes also having type 3 clasts) contain foreign fragments completely unrelated to the host rock main lithology. These, e.g., include achondritic (granite-like) clasts in Adzhi-Bogdo (stone; LL3-6), an andesitic lithology in Study Butte (H3-6), and a unique fragment with affinities to winonanites within the brecciated Villalbeto de la Pena (L6) (Bischoff et al., 1993a, 2013a; Sokol et al., 2007a,b; Terada and Bischoff, 2009; Dyl et al., 2012). During this study, clasts of different chondrites in Krymka (LL3; Fig. 5a) and Sahara 98645 (H3; Fig. 5d; volatile-rich, CI-like clast; Patzek et al., 2018), a heavily-recrystallized (type 5/6) fragment in Adrar 003 (LL3.1; Fig. 5c), and graphite-bearing clasts with affinities to ureilites in Adrar 003 (Fig. 5b) and NWA 5697 (L3) have been found. Although differences in mineralogy of these clasts and the host meteorite are noticeable, oxygen isotope analyses of olivine grains in these clasts help to determine their genetic relationships. The olivine grains in the graphite-bearing clasts in Adrar 003 and NWA 5697 have very similar oxygen isotopic composition ($\Delta^{17}O$ ranging from -0.36 to -1.47) compared to bulk ureilites and the ALM-A trachyandesite from the Almahata Sitta meteorite strewn field (Bischoff et

al., 2014; Table 2; Fig. 6). One olivine grain from the CI-like clast in Sahara 98645 plots slightly above the CCAM ($\Delta^{17}O$=-2.14 ‰; Fig. 6; for mineralogy see Patzek et al. (2018)) and the phyllosilicate-rich areas are slightly more enriched in $^{17}O$ compared to bulk CI chondrites ($\delta^{18}O \approx 17$ ‰; $\delta^{17}O \approx 11$ ‰; Fig. 6). The data of the phyllosilicate analyses are less precise due to possible matrix effects and missing proper SIMS standards.

### 3.3. Abundance and location of shock veins

Parallel to the search for features of brecciation, shock veins (generally planes in three dimensions) in the H, L, and LL chondrites were also registered. Some typical examples are given in Fig. 7. Considering the heavily-brecciated LL chondrites, in 63 of the 140 (45%) examined LL chondrites shock veins were clearly detected. 57 of these 63 chondrites are brecciated rocks. 63% of the LL6 chondrites contain shock veins. The investigation of the H and L chondrites has shown that about 26% (310 of 1193) of the H chondrites and 40% (379 of 947) of the L chondrites contain shock veins (Table 1; Fig. 7). In all petrologic types, the L chondrites have a higher abundance of shock vein-bearing rocks than the H chondrites. Concerning the occurrence of shock veins, large differences between the two groups can be noticed for the petrologic type 3 and type 6 chondrites (H3: 15% veined, H6: 34% veined; L3: 30% veined, L6: 47% veined). The abundances of shock vein-bearing type 5 chondrites is very similar in all chondrite groups (~30%). Considering the shock vein-bearing rocks in both chondrite groups (H, L), most of the shock veins occur in unbrecciated meteorites. However, considering the abundance of shock veins in brecciated rocks a significant difference between chondrites of low petrologic types (3 and 4) and those of high petrologic types (5 and 6) is noticeable. In the H chondrites more than half of the shock veins occur in brecciated meteorites of petrologic type 3 and 4 (88% and 51%, respectively), while in petrologic type 5 and 6 chondrites only 40% and 36% of the shock vein-bearing rocks, respectively, are brecciated. The same trend is visible for the L chondrites. Among the L3 and L4 chondrites 92% and 68%, respectively, of the vein-bearing rocks are breccias, while among the brecciated L5 and L6 chondrites only 37% and 26%, respectively, have shock veins.

About half of the brecciated chondrites (H chondrites: 48%; L chondrites: 61%; LL chondrites: 52%) contain shock veins. In general the number of ordinary chondrites with shock veins increases with the petrological type. In all chondrite groups the type 6 chondrites have the highest percentage of shock veins and this significant aspect will be discussed below in more detail.

Another important aspect that was examined is the location of the shock veins within a meteorite as presented in Fig. 7. Table 1 distinguishes between the abundance of shock veins cutting through the

whole meteorite and the abundance of shock veins that are locally limited to individual fragments (Figs. 7c, 7d, 7f). Some examples of shock veins penetrating through the entire rocks are shown in Figs. 7a,b,e from Villalbeto de la Pena, Ardon, and Chelyabinsk (Bischoff et al., 2013b; Trigo-Rodriguez et al., 2014; Morlok et al., 2017). In the H chondrites about 94% of the shock veins crosscut the whole meteorite including diverse fragments. Only 6% of the shock veins are locally limited to distinct clasts. Among the shock vein-bearing L chondrites in ~91% of the rocks the shock veins crosscut the whole meteorite and only in 7% of the cases the shock veins are locally limited to fragments. The low percentage of shock veins that are limited to fragments in the L chondrites is due to the fact that (a) the percentage of breccias is low and (b) a large number of L6 chondrites have shock veins and these veins crosscut the entire rocks. In 40% of the LL chondrites the shock veins are restricted to individual fragments. Examples are shown in Figs. 7c,d,f. Thus, the abundance of chondrites with shock veins restricted to individual fragments is clearly related to the abundances of breccias and has important implications concerning the shock and fragmentation history of the rocks (see below in the discussion).

### 3.4 Impact melt breccias and impact melt fragments in ordinary chondrites

Impact melts are the product of high stress (above 75-90 GPa) and temperature (above 1500-1750 °C) induced by impact processes (Stöffler et al., 1991). Due to these extreme conditions, the target lithology gets partially or completely molten (e.g., Keil, 1982; Takeda et al., 1984; Stöffler et al., 1988, 1991; Yamaguchi et al., 1998, 1999; Mittlefehldt and Lindstrom, 2001; Bischoff et al., 2006). However, unmolten clasts of the host lithology can survive in the melt. On the asteroid the melt quickly cools down (e.g., Rubin and Moore, 2011) and forms a new melt lithology. Alternatively, fragments of the melt can be excavated and/or ejected in order to reach other areas of the parent body or other regions in the solar system and, consequently, accreted onto other bodies. These melt fragments can give information about the parent lithologies of the source planetesimals as well as about processes of mixing, re-accretion, and re-lithification of the newly-formed body(ies). During the present investigations 17 ordinary chondrites were classified as impact melt breccias (Table 3). In these cases the melt lithology of the studied thin sections makes up the dominant part of the rock embedding fragments of the target materials. These clasts are in most cases of type 6 chondritic materials; however, nothing can be said, if the fragments represent target materials or the projectiles. Our thin sections of Chico and Shaw (both L6), previously described as impact melt breccias (Taylor et al., 1979; Bogard et al., 1995; Norman and Mittlefehldt, 2002) do not show any

characteristics for being breccias and are not regarded as impact melt breccias in this study. In addition to the impact melt breccias, within 55 brecciated chondrites fragments of impact melt were found. Table 3 lists only the samples with unambiguously-identified melt clasts. For small melt clasts the identification is often somewhat unclear based on optical similarities with textures in porphyritic chondrules or chondrule fragments.

As described above, impact melts have an igneous texture and consist of euhedral to subhedral olivine and pyroxene grains embedded into a fine-grained (or glassy) mesostasis due to fast cooling of the melt (Stöffler et al., 1991). Furthermore, these minerals are often zoned (Fig. 8a), which indicates distinct stages of mineral growth. In the beginning of the cooling process, olivine and pyroxene grains with a relatively high Mg concentration start to crystallize. Due to continuous growth of these Mg-rich minerals and the subsequent depletion of Mg in the melt, the melt becomes enriched in Fe leading to Fe-enrichment in the rims of olivine and pyroxene grains compared to their cores (Fig. 8a). Variable Fe-Mg concentrations within silicates of the melt rocks represent disequilibration due to the chemical conditions during crystal growth from a melt (Van Kooten and Buseck, 1978). This process is similar to magmatic crystallization on Earth. Another characteristic feature of impact melts is the existence of droplets of immiscible sulfide and Fe-Ni metal (Fig. 8f).

### 3.5 Noble gas data

Noble gas data are available for only about 12% of the meteorites studied here. Nevertheless, the existing noble gas data are a very valuable addition to define the type of chondritic breccia and the setting of its constituents. It can safely be assumed that noble gases with solar-like elemental and isotopic compositions in a bulk ordinary chondrite sample indicate trapping of noble gases from the solar wind in the regolith of a parent body. Solar noble gases therefore indicate a regolith breccia. On the other hand, cosmogenic noble gases produced by interactions of high energy cosmic ray protons and alpha particles with target atoms within the first very few meters of the surface of a body have the potential to reveal the mixing history of an asteroidal regolith (e.g., Wieler et al., 1989a,b). Distributions of cosmic-ray exposure ages of meteorite classes may tell us about the large-scale break-up and reassembly history of parent bodies (e.g. Crabb and Schultz, 1981; Graf and Marti, 1995). Cosmic ray exposure ages and presence or absence of solar noble gases of the meteorites studied here are indicated in the Table A1 (supplement). The majority of the exposure ages are taken from the compilations by Marti and Graf (1992) and Graf and Marti (1994, 1995). Additional ages in Table A1 are based on more recent noble gas data (for details see explanations to Table A1 in Chapter 2.2).

Tables 4 and 5 confirm the well-known disparity of the fractions of solar gas-bearing meteorites among the different OC groups. In our data-set 20% of the H chondrites and 8.3% of the LL chondrites but only 3.0% of the L chondrites contain solar noble gases. For the two larger groups (H and L chondrites), these data compare reasonably well with those given in earlier (and larger) compilations by Crabb and Schultz (1981) and Graf and Marti (1995). This agreement is, of course, no surprise, given that all compilations are based to a large part on the same data. The difference of almost a factor of 2 in the fraction of LL chondrites listed as solar gas-rich here and by Graf and Marti (1994), respectively, is certainly not relevant given the poor statistics (three gas-rich meteorites in each compilation).

A remarkable difference is observed in the fraction of brecciated meteorites with solar noble gases in the three groups (Tables 4 and 5). About 62% of all brecciated H chondrites with noble gas data contain solar noble gases, compared to only around 11% and 10% of the brecciated Ls and LLs, respectively. Thus, about two thirds of all brecciated H chondrites but only one out of 10 brecciated Ls and LLs are regolith breccias. Although statistics are poor, the fraction of regolith breccias apparently is similarly high in all petrologic types of the H chondrites (Table 4), an observation already made earlier (Crabb and Schultz, 1981; Graf and Marti, 1995).

The observations on trapped noble gases can thus be summarized as follows: solar-gas rich regolith breccias are considerably more abundant in the H group than in the other two groups, irrespective of whether the entire respective groups or only the brecciated subsets are considered. The well-known scarcity of solar-gas-rich L chondrites is also observed here.

It is well-known that cosmic ray exposure ages of groups of meteorites are not uniformly distributed, but show distinct peaks, which indicate major collisional events on the respective parent bodies (Crabb and Schultz, 1981; Marti and Graf, 1992; Graf and Marti, 1994, 1995). The number of available exposure ages in our data set is rather limited, however; in particular not allowing to evaluate whether exposure age distributions of brecciated and unbrecciated meteorite subsets may differ from each other. In the Discussion section below we will largely rely on earlier work (Crabb and Schultz, 1981; Graf and Marti, 1994, 1995).

Here, we just highlight one observation in our dataset concerning the most remarkable of all peaks in exposure age histograms. Almost half of all H chondrites display a cosmic ray exposure age around ~7 Ma (e. g., Anders, 1964; Graf and Marti, 1995), indicating that one collision (or perhaps two, cf. Graf and Marti, 1995) in the asteroid belt ~7 Ma ago is responsible for about 20% of all meteorites falling to Earth today. While it was noted early on that this exposure age peak

encompasses H chondrites of all petrologic types (e. g., Wänke, 1968), Zähringer (1968) first noted that the 7 Ma peak was particularly pronounced in the H5 type. This preponderance was confirmed by Crabb and Schultz (1981) and Graf and Marti (1995), and the latter authors also noted a similarly-marked peak for H4 chondrites but shifted by about 1 Ma towards higher ages. Types 3 and 6, on the other hand, display only subdued ~7 Ma peaks. In our data-set (which contains about twice as many H3 chondrites than that of Graf and Marti, 1995) we qualitatively confirm the observations by these authors (Table A1). Only about 27% of the H3 chondrites (12 of 45) and 29% (6 of 21) of the H6 chondrites have exposure ages falling into the "7 Ma peak" (loosely-defined here as encompassing ages between 4.5 - 7.5 Ma). On the other hand, 24 of 49 H5s (49%) and 7 of 18 (39%) of the H4 chondrites have nominal exposure ages between 4.5 and 7.5 Ma, respectively. While these figures need to be taken with a grain of salt (due to the limited accuracy of nominal exposure ages as well as the rather loose definition of the width of the "7 Ma" peak) it appears clear that the proportion of the H chondrites that were ejected in the big collision(s) around 7 Ma ago is larger for types H5 and H4 than for H3s and H6s.

## 4. DISCUSSION

### 4.1. Comparison of values of this work with data of Binns (1967) and Scott et al. (1989)

While Binns (1967) found that about 33% of the H chondrites (named olivine-bronzite chondrites in that work) are brecciated, this study shows a significantly lower abundance of brecciated H chondrites (23%), which is similar to the data obtained by Scott et al. (1989; 24%). For the L chondrite group (named olivine-hypersthene chondrites by Binns (1967), Binns determined an abundance of 20% brecciated L chondrites, which is similar to the results of this study 23% and to that of Scott et al. (1989) with 18%. For LL chondrites (Binns: amphoterites) Binns (1967) assumed an abundance of 65% of brecciated chondrites (Scott et al.: 58%), while here we determined an abundance of 79% (see also Schleiting and Bischoff, 2015, 2017). However, the data of Scott et al. (1989; 24% H, 18% L, 58% LL) are indicated as lower limits.

Hence, the general trend is similar in all three studies: The LL chondrite group contains by far more brecciated chondrites than the H and L groups. The small, but recognizable differences between the results of this study and those of Binns (1967) and Scott et al. (1989) could have several reasons:

(a) First of all the number of investigated chondrites differs drastically. While Binns (1967) investigated 361 ordinary chondrites (148 H chondrites, 184 L chondrites and 29 LL chondrites), in this study 2280 (1193 H chondrites, 947 L chondrites and 140 LL chondrites)

were investigated. Therefore, the statistical errors in Binns` study should be larger than in this study. A precise number of studied samples is not given by Scott et al. (1989; n>250).

(b) Another aspect that could lead to these differences is the substantial number of hot desert meteorite finds that were microscopically investigated in this study. In 1967, Binns could not yet have investigated many meteorites from desert dense collection areas, as most meteorites from the Sahara and other hot deserts have been found since 1989 (e.g., Bischoff and Geiger, 1995).

(c) Most of the meteorites studied here as well as by Binns (1967) and probably also those by Scott et al. (1989) are finds. Due to weathering, the meteorites are clearly modified by terrestrial processes. Fluids have changed the interior mineralogy, metalswere oxidized to Fe-hydroxides, and veins of terrestrial alteration products (calcite, Ca- and Ba-sulfate) formed. Such alteration processes can lead to significant changes in the appearance of the rocks. This is especially the case for the H-chondrites. Based on the high metal content of fresh H chondrites weathering leads to inhomogeneous formation of rust and other alteration products within the meteorite finds. This can lead to the impression of having a brecciated rock with fragments of different brownish taints. Thus, in thin sections it is difficult in many cases to unambiguously testify a highly-weathered rock as a true breccia.

(d) During the microscopic studies it became obvious that H3 and H4 chondrites contain many more mineral and chondrule fragments than L and LL chondrites of similar petrologic type. However, a clear brecciated texture was difficult to attest for these H-chondrites of low petrologic types. In this case to decide “for” or “against” a brecciated rock is a very subjective decision. Perhaps, the mineral and chondrule fragments existed already as clasts during accretion.

Problems of pairing and sectioning complicate interpretations. Often meteorites break up in the atmosphere resulting in meteorite showers in a strewn field. Good recent examples are the meteorite showers of Almahata Sitta and Chelyabinsk in which thousands of different fragments reached the surface. As desert areas accumulated meteorites over thousands of years it is not always clear at all, which fragments originate from the same meteoroid entry into the Earth atmosphere. Due to weathering, the meteorite gets modified and a clear relationship between samples of a common fall is difficult to diagnose. This effect of possible pairing of meteorites could have an important impact on the results of this study. The total number of investigated meteorites would be changed as well as the numbers for the abundance of breccias and shock vein-bearing chondrites. However, the error

due to pairing is likely very small as already suggested by Schleiting and Bischoff (2017). As an example the abundance of brecciated meteorites in the LL chondrite group without taking pairing into account is ~79% (based on studying 140 LL chondrites). After excluding samples from dense collection areas the abundance of brecciated meteorites is about 78% (Table 1). Similar results were obtained in this study considering the H and L chondrites (Table 1). The quantity of breccias in unpaired (dense collection areas excluded) H and L chondrites is about 21% and 19%, respectively. These values are similar to the obtained results including hot desert meteorites (H chondrites: 23%; L chondrites: 23%; Table 1).

It is important to mention the size of the PTS. The largest PTSs are about 8 $cm^2$. Still, it is uncertain, how far these sections represent the whole meteorite and, consequently, the parent asteroid. The PTS could represent a small fragment with a completely different lithology than most parts of the actual parent body. This problem is described in detail above and demonstrated by Fig. 1. Different modes of observations may also be responsible to lead to differences in the abundance of registered breccias between the works of Binns (1967), Scott et al. (1989), and this study. In this respect, two fundamental questions are: Are chondrites with networks of shock veins breccias or not? When should such a rock be classified as a monomict breccia (compare Fig. 1)?

### 4.2. Different abundances of brecciated rocks among the H, L, and LL chondrite groups - indications for a different evolution of parent bodies?

The LL chondrites are by far the most heavily brecciated class among the ordinary chondrites. This fundamental result is consistent with earlier studies by Binns (1967) and Scott et al. (1989).

The differences in the individual groups of the ordinary chondrites indicate a different formation and impact history for the parent bodies of H, L, and LL chondrites. The similar abundance of brecciated meteorites among the H and L chondrites might be viewed to indicate a similar impact frequency on their parent bodies, in contrast to a supposedly higher impact frequency on the LL parent bod(y)ies. One might thus ask whether the abundance of brecciated chondrites in a group may somehow correlate with the abundance of a) solar gas-rich regolithic meteorites and/or b) the cosmic ray exposure age distributions.

Concerning the first possibility (a) this is obviously not the case. The LL chondrites - being the group with the highest percentage of brecciated members - has the lowest fraction of regolithic meteorites. The H and L chondrites have a similar fraction of brecciated meteorites, but the percentage of regolith breccias is almost 5 times higher in H chondrites than in L chondrites. These

observations indicate that the formation history of brecciated meteorites is largely decoupled from the formation history of parent body regoliths. This conclusion is also strongly supported by the exposure age distributions, as discussed in the next paragraph.

The cosmic ray exposure age distributions of all three groups of ordinary chondrites show several more or less pronounced clusters. The most prominent one at ~7 Ma in the H chondrite histogram has already been mentioned in Chapter 3.5. In addition, the H chondrite histogram shows smaller clusters at 33 Ma and 24 Ma (Graf and Marti, 1995), whereas the L chondrite histogram shows a marked peak at 40 Ma (followed by a sharp drop-off towards higher exposure ages) and a smaller peak at 28 Ma (Marti and Graf, 1992). About one third of the LL chondrites have exposure ages close to 15 Ma and smaller clusters at 28 Ma and 40 Ma in the LL chondrite histogram are also observed. The latter clusters coincide with those of the L chondrites. All these clusters indicate major collisional events in the asteroid belt. Apart from this basic observation, arguably the most remarkable fact about these histograms is that most of the peaks occur in several or even all petrologic types of the respective meteorite group, although the peaks are not equally conspicuous in all types. For example the 7 Ma H chondrite peak is more prominent in meteorites of petrologic types 5 and 4 than in those of types 3 and 6 (Graf and Marti, 1995). Similarly, the 15 Ma event is more pronounced in the histograms of the LL5 and LL6 chondrites than in the LL3 and LL4 chondrites (Graf and Marti, 1994).

The most straightforward explanation of the presence of several petrologic types in the same exposure age peak is that the immediate (last generation) respective parent body does not retain a presumed original layered structure (with petrologic type 3 representing the outermost layer and higher types consecutively deeper layers (e.g., Pellas and Storzer; 1981; Göpel et al., 1994; Trieloff et al., 2003)). Instead, the original parent body catastrophically fragmented and subsequently reassembled into a mega breccia (Davis and Chapman, 1977; Anders, 1978; Crabb and Schultz, 1981). The variable abundance of meteorites of different petrologic types in a peak likely indicates that the mega breccia of the last generation parent body is not completely mixed either laterally or vertically (Crabb and Schultz, 1981). In this picture it becomes obvious that the global brecciation history of a meteorite group is largely independent of the regolith formation history of its (last) parent body. This also implies that solar wind implantation on parent bodies is an ongoing process (Crabb and Schultz, 1981). Otherwise, if the parent body had been irradiated predominantly before the mega breccia formation, meteorites of petrologic type 3 (and 4?) would contain a much higher fraction of solar gas-rich members than higher types, contrary to observation for H chondrites, where statistics allow a meaningful statement (see Chapter 3.5).

At first sight one observation speaks against the idea that the global brecciation history of a meteorite group is largely independent of petrologic type: while only about 20% of the H4, H5, and H6 chondrites of our samples are brecciated (Table A1), about two thirds of the H3 chondrites are classified as breccias, in contrast to the observation that solar gas-rich regolith breccias are roughly equally abundant among all petrologic types. However, the reason for this is probably due to the fact that among the type 3 chondrites also those breccias are listed in which the fragments of higher petrologic types 5 and 6 are dominating (H3-5, H3-6). This probably does not speak against an early global fragmentation and brecciation, it may indicate a local impact-induced mixing of components perhaps long after the mega breccia formation.

An inference about the timing of major brecciation events can be made for the L chondrites based on their $^{4}$He and $^{40}$Ar records. Many L chondrites are severely depleted in radiogenic $^{4}$He and $^{40}$Ar as a result of significant heating following a large collision in the asteroid belt (Bogard, 1995), which presumably led to the break-up of an L chondrite parent body ~470 Ma ago (Korochantseva et al., 2007). Marti and Graf (1992) note that the two less prominent exposure age clusters of the L chondrites at 28 Ma and 5 Ma appear to be dominated by poor $^{40}$Ar retainers (i. e. $^{40}$Ar <4000*10$^{-8}$ cm$^{3}$STP/g), and suggest that these events indicate fragmentation of a parent body which earlier had suffered catastrophic out-gassing. In our data set (Table A1) 18 brecciated L chondrites are poor $^{40}$Ar retainers and 10 have "normal" $^{40}$Ar (>4000**10$^{-8}$ cm$^{3}$STP/g). This proportion of ~64% of $^{40}$Ar-poor brecciated members is very similar to the overall fraction of ~66% of $^{40}$Ar-poor L chondrites studied by Marti and Graf (1992). Since about one third of the breccias did not experience degassing, much earlier brecciation events on L chondritic asteroids are required prior to the catastrophic break-up of the remaining L parent body some 470 Ma ago. The fact that only a small fraction of ~3% of the L chondrites are solar-gas-rich regolith breccias (compared to some 15% of the H chondrites; Table 5) may well also be related to the parent body break-up event 470 Ma ago. Crabb and Schultz (1981) note two possibilities. Either only small layers of fresh regolith may have developed on the (small, low gravity) post-break-up last generation parent bodies of the $^{40}$Ar-poor L chondrites, or the solar gas-free L chondrites stem from last generation parents which had lost all solar gases and most radiogenic gases upon break-up. Crabb and Schultz (1981) suggest that the few solar-gas-bearing L chondrites seem not to belong to the group of $^{40}$Ar-poor retainers, which is confirmed here, since all three solar-gas rich L chondrites listed in Table A1 (Acfer 066, Assam, NWA 869) have "normal" $^{40}$Ar concentrations. This observation appears to favour the second possibility.

Graf and Marti (1995) note that the 33 Ma event in the H chondrite exposure age histogram may actually represent a considerably larger collisional event than that resulting in the more prominent 7 Ma peak, since the mean life of meteorite-sized bodies is only on the order of 10 Ma. These authors therefore suggest that the 33 Ma collision may have been large enough to sample most or all petrologic types even on a parent body with more or less intact layered structure. Yet, as emphasized further up in this section, the overall conclusion is that the events leading to the ejection of meteoroids from a last generation parent body as they are reflected in the cosmic ray records of the different ordinary chondrite groups are largely decoupled from the major events that resulted in the brecciated ordinary chondrites.

### 4.3. Impact melt clasts and the evolution of the parent body

Ordinary chondrite impact melt breccias or clasts of impact melt breccias in H, L, and LL chondrites offer direct evidence for high-energy collisions. Impact melt breccias are well-known among the L-chondrites: e.g., Ramsdorf, Madrid, Point of Rocks, PAT 91501 (e.g., Nakamura et al., 1990b; Casanova et al., 1990; Yamaguchi et al., 1999; Mittlefehldt and Lindstrom, 2001; Raack, 2007). Dar al Gani 896, Spade, and Smyer can be regarded as H-chondrite impact melt breccias (Folco et al., 2002; Rubin, 2002; Burbine et al., 2003; Rubin and Jones, 2003) and the Portales Valley rock is seen as an annealed impact melt breccia (Rubin et al., 2001) that was subsequently buried and cooled at 6.5 K/Ma (e.g., Kring et al., 1999; Sepp et al., 2001). The Antarctic LL chondrites Yamato-790964 and -790143 are listed as impact melt rocks, which represent nearly total melting of precursor rocks (Sato et al., 1982; Okano et al., 1990; Yamaguchi et al., 1998).

The appearance of the impact melt itself as well as the composition of the olivine and pyroxene as newly-crystallized constituents give valuable information about the host lithology of the melt (e.g., unmelted fragments within the melt; Fig. 8a) and also on parent body processes (e.g., later annealing) that followed the melt rock formation. During annealing processes (metamorphism, perhaps triggered by impact) the chemical composition of the zoned phases within the impact melts (Fig. 8a) may equilibrate and inherit the composition of the new brecciated lithology or the rocks of the newly-accreted daughter parent body. An example is shown by the impact fragment from NWA 2443 (H3-6; Fig. 8b). Only a very small range of Fa and Fs contents in the olivine and pyroxene grains, respectively, is documented as well as the absence of distinct zoning in minerals of the impact melt fragment. This is clear evidence for an annealed rock (Fig. 8b) and must be the result of

thermal metamorphism (annealing) experienced by the melt fragment after melt rock formation. Interestingly, NWA 2443 (H3-6) also contains clasts of impact melt breccias that are completely unequilibrated (Fig. 8a) having strongly-zoned grains of olivine and pyroxene. Consequently, both types of impact melts have experienced a different evolution. Those impact melt lithologies with equilibrated silicates must have been buried and annealed after melting and crystallization in order to equilibrate. Parts of these melts must have been excavated by impact and were subsequently mixed with other chondritic clasts including impact melt lithologies with unequilibrated silicates in near-surface locations of the parent body, were lithified by shock, and ejected as polymict breccias (Kieffer, 1975; Bischoff et al., 1983). Thus, these re-accreted and re-lithified rocks certainly represent an impact-induced, second-generation parent body lithology and demonstrate that several distinct collisional events are necessary in order to form this kind of breccias with melt rock clasts having different characteristics.

### 4.4. Simultaneous accretion of asteroidal clasts and chondrules and formation of complex breccias

That certain meteorites represent samples of "second-generation" parent bodies (daughter asteroids) formed after collisional destruction of primordial, first generation, "grandparent" planetary bodies has been discussed earlier (e.g., Urey, 1959, 1967; Zook, 1980; Hutchison et al., 1988; Hutchison, 1996; Sanders, 1996; Bischoff, 1998; Bischoff and Schultz, 2004; Bischoff et al., 2006, 2010; Sokol et al., 2007a; Horstmann et al., 2014; Horstmann and Bischoff, 2014; Weyrauch et al., 2018).

Evidence for the existence of planetesimals before the accretion of the parent asteroids of chondrites have been provided by W isotope data for iron meteorites (e.g., Kleine et al., 2004, 2005, 2008).
In this respect primitive, accretionary breccias can be formed in a low velocity regime and mainly occur among carbonaceous and ordinary chondrites (e.g., Kracher et al., 1982; Scott and Taylor, 1982). They consist of chondrules as well as different types of (sometimes foreign) fragments (compare Fig. 5). Considering various types of clasts in carbonaceous and ordinary chondrites, Bischoff and Schultz (2004) suggested that many breccias result from mixing of fragments after total destruction of precursor parent bod(y)ies. They also assumed that dark inclusions in CR and CH chondrites (compare Patzek and Bischoff, 2015; Patzek et al., 2016) may be excellent witnesses to document formation of the final parent body by secondary accretion. In this study, xenolithic fragments were also encountered in some accretionary type 3 breccias (see above; Fig. 5) and other chondrite breccias. Examples are Glanerbrug (as mentioned before; Niemeier and Bischoff, 2006)

and Villalbeto de la Pena (L6 breccia with a winonaite-related clast; Dyl et al., 2012; Bischoff et al., 2013a), Krymka (LL3; e.g., Semenenko et al., 2001; Bischoff et al., 2006; Fig. 5), Sahara 98645 (H3, Fig. 5) and Adrar 003 (LL3; Sokol et al., 2007a; Fig. 5).

The presence of xenolithic fragments in ordinary chondrites has been known for several decades. A significant number of reports about clasts in ordinary chondrite breccias exist that are unrelated to the host meteorite. These clasts can be of chondritic and achondritic origin, must have been ejected from their first generation parent body, and incorporated into the present breccias (e.g., Dodd, 1974; Fodor and Keil, 1975, 1976, 1978; Schultz and Signer, 1977; Keil, 1982; Rubin et al., 1982, 1983, 2005; Prinz et al., 1984; Hutchison et al., 1988; Christophe Michel-Lévy, 1988; Wieler et al., 1989a,b; Rubin, 1989, 1997; Nakamura et al., 1990a; Misawa et al., 1992; Kennedy et al., 1992; Bischoff et al., 1993a, 1997; MacPherson et al., 1993; Nagao, 1994; Mittlefehldt et al., 1995; Bridges et al., 1995; Ruzicka et al., 1995, 1998; Bridges and Hutchison, 1997; Vogel et al., 2003; Hezel, 2003; Rubin and Bottke, 2009; Gattacceca et al., 2017).

Complex breccias with a huge variety of xenolithic clasts like Kaidun and Almahata Sitta (Ivanov, 1989; Zolensky and Ivanov, 2003; Bischoff et al., 2010; Goodrich et al., 2014; Horstmann and Bischoff, 2014) were not encountered in this study. However, some ordinary chondrite breccias also contain a huge variety of parent body lithologies as well as xenoliths. Good examples are Adzhi-Bogdo (stone) and NWA 869 (e.g., Bischoff et al., 1993a, Metzler et al., 2011). NWA 869 (L3-6) contains unequilibrated and equilibrated chondrite clasts, some of which display shock-darkening, impact melt rocks (IMRs; both clast-free and clast-poor), unequilibrated microbreccias, two different types of light inclusions, and different $SiO_2$-bearing objects (Metzler et al., 2011). The Adzhi-Bogdo (LL3-6) chondrite regolith breccia contains various types of fragments: highly recrystallized clasts (sometimes with internal shock veins), melt rock clasts, fragmental breccia clasts, shock-darkened fragments as well as xenolithic L chondrite and achondritic clasts including granite-like lithologies (Bischoff et al., 1993a, 1996; Terada and Bischoff, 2009). Considering the achondritic lithologies in Adzhi-Bogdo and the trachyandesite described by Agee et al. (2018), which has a similar O-isotope composition compared with those of ordinary chondrites and of the granitic clasts (Sokol et al., 2007b) it has to be suggested that igneous processes occurred on the LL chondrite parent body or on a separate planetesimals within the same oxygen isotope environment. The occurrence of graphite-bearing clasts within the ordinary chondrites Adrar 003 and NWA 5697

and their oxygen isotopic composition linking them to ureilitic material is another evidence for complex mixing of isotopically different materials.

### 4.5. Parent body processes - breccias and the formation of shock veins

The abundance of chondrites that contain shock veins (or planes in three dimension) weakly correlates with the abundance of brecciated chondrites among the ordinary chondrite classes. The abundances of meteorites that contain shock veins in the H, L, and LL chondrites are about 26%, 40%, and 45%, respectively, and the corresponding abundance of brecciated H, L, and LL chondrites is 23%, 23%, and 79%, respectively (Table 1). As noted above for the ordinary chondrite bulk rocks, the substantial number of LL chondrites with shock veins indicates that many more impacts may have affected the LL chondrite parent body/bodies and modified the present (especially surface) lithologies. These processes have led to repeated impact-related excavation of material, mixing, and breccia formation. A good argument is the observation that LL chondrite breccias contain abundant clasts (~40%, as discussed below), in which the shock veins are limited to individual clasts. This feature indicates that several impact processes are necessary to obtain this textural characteristic.

Considering the abundance of breccias among the H and L chondrites, which is almost equal, the abundance of meteorites with shock veins differs between these two chondrite groups (Table 1). If there is a direct correlation between the abundance of shock veins and breccia formation, then, the abundance of breccias among the L chondrites should be somewhat higher than the number of breccias in this group.

Considering all shock vein-bearing chondrites most chondrites with veins are of petrologic types 5 and 6 (together: 626 chondrites) compared with those of petrologic types 3 and 4 (125 ordinary chondrites). This is in part due to the fact that the H5 and L6 chondrites are the most abundant classes of meteorites. Considering all 2280 studied chondrites this correlation – although weak – can still be diagnosed: About 30% of the H5 and H6 and ~17% of the H3 and H4 chondrites have shock veins (L: 43 vs. 30%; LL: 47 vs. 38%).

The relationship between the petrologic type and the abundance of shock vein-bearing H, L and LL chondrites can be best explained with an early mega breccia formation which is in agreement with noble gas data previously discussed (e.g., Davis and Chapman, 1977; Anders, 1978; Crabb and Schultz, 1981). If the shock vein-forming impacts would happen on an onion shell-like body, most shock veins should be found in rocks of low petrologic types (types 3 and 4), which are more porous than the compact rocks of high petrologic type and which are located in outer parts (at the

surface) of the meteorite parent body. Stöffler et al. (2018) clearly point out that the probability for the formation of shock veins and shock melts is significantly higher in porous rocks with variable density (i.e., variable shock impedance) than in compact rocks from deeper locations. This contrasts with the results of this study and with those of Schleiting and Bischoff (2015). Most of the H, L, and LL chondrites that contain shock veins belong to the petrologic types 5 and 6. Therefore, these type 5 and 6 lithologies must have been excavated by a catastrophic impact event from the interior of the parent body to its surface. Thus, this could be taken as an indicator for the complete destruction of each of the original parent bodies of the H, L, and LL chondrites.

Most of the shock veins in ordinary chondrites crosscut the whole meteorite and are not limited to single fragments (Fig. 7). However, the LL chondrites again differ from H and L chondrites. The amount of shock veins that are limited to fragments is much higher in LL chondrites (~40%) than in the H (~6%) and L (~7%) group ordinary chondrites. The observation of abundant LL chondrite breccias with shock veins limited to individual clasts (~40%, as stated before) clearly indicates that second-generation bodies must have formed and existed. After a shock event producing shock veins, a breakup of the LL chondrite parent body (or parts), with subsequent re-accretion and re-lithification is required in order to explain these shock features within the brecciated parent asteroid(s).

### 4.6. Evolutionary history of chondrite parent bodies

#### 4.6.1. In the beginning

The history and evolution of the ordinary chondrites and their components started with (a) the formation of Ca,Al-rich inclusions (CAIs; e.g., Chen and Wasserburg, 1981; Amelin et al., 2010; Connelly et al., 2012; MacPherson, 2014), (b) formation and evolution of chondrule precursor components (including early-processed relict minerals (perhaps the relict olivines; e.g., Rambaldi, 1981)), (c), melting of dust aggregates and formation of chondrules (e.g., Kita et al., 2005; Connelly et al., 2012), (d) the transport of small CAIs into the accretion region of ordinary chondrites (Ebert et al., 2017), (e) transport of xenoliths as those described in Chapter 3.2 and shown in Fig. 5 into the accretion area, which was followed by rapid accretion of the ordinary chondrite parent bodies. All these processes probably happened within a time range of ~2 Ma (e.g., Kleine et al., 2008; Connelly et al., 2012; Vernazza et al. 2014; Blackburn et al., 2017).

It is very often considered that each of the three groups of ordinary chondrites derives from only one “primordial” asteroid as it existed in the first tens of Ma of solar system history (e.g., “the H chondrite parent body”), often without explicit discussion of this assumption (e.g., Trieloff et al., 2003, Blackburn et al. 2017). However, Burbine et al. (2002) highlight the enormous disparity between the presumed 100 - 150 meteorite parent bodies sampled on Earth and the ~1,000,000 asteroids in the main belt > 1 km. They mention that no direct evidence rules out multiple primordial chondritic asteroids of essentially identical material. Vernazza et al. (2014) suggest that large groups of compositionally similar asteroids are a natural outcome of planetesimal formation. Consequently, meteorites within a given class can originate from different parent bodies. One may also ask in this context why the iron meteorites should represent ~70 different (primordial) parent bodies (Wasson, 1995) but the ordinary chondrites only three, even given the longer lifetimes against destruction of the former due to greater material strength as manifested by their longer cosmic ray exposure ages (Herzog and Caffee, 2014). Burbine et al. (2002) also mention that a single original parent body may have produced large numbers of current asteroids. As discussed above, cosmic ray exposure age distributions of meteorites largely reflect ejection events from these “last generation parent bodies” as we call them in this paper in contrast to the “primordial” or “first generation” parent bodies.

### 4.6.2. Fragmentation and formation of asteroid families

In general, the fragmentations, which are strictly required to explain various kinds of analytical data and distinct textural and mineralogical observations (e.g., Taylor et al., 1987; Bischoff et al., 1993a, 2006; Keil et al., 1994; Scott, 2002; Davidson et al., 2013; Blackburn et al., 2017; see further discussion below), must be considered to have occurred sometime after the formation of the early, first-generation parent bodies. It is clear that impacts controlled the formation of asteroids as well as their destruction and were a major factor in their planetological evolution (Scott et al., 1989; Scott, 2002).

Starting with the accretion of first generation ordinary chondrite parent bodies ~4.56 billion years ago, fragmentation processes until today have led to the formation of complex re-accreted parent bodies (e.g., Davis and Chapman, 1977; Taylor et al., 1987; Scott et al., 1989; Keil et al., 1994; Scott, 2002; Bischoff et al., 2006; Davidson et al., 2013; Blackburn et al., 2017). By dating

techniques the formation of impact melt or other shocked rocks on ordinary chondrite parent bodies is recorded (e.g., H chondrite: events at 3630 Ma (Keil et al., 1980) and ~1400 Ma (Schultz and Signer, 1977); L chondrite: events at 1790 and 2216 Ma (Metzler et al., 2011).

Catastrophic collisions led to later generation asteroids, some of which may still be recognized as "families" with similar orbits (e.g. Hirayama, 1918; Zappalà et al., 2002; Vernazza et al., 2014, McGraw et al., 2018). It is suggested that collisional and dynamical modeling indicate that groups of meteorites producing numerous falls would more likely derive from asteroid families than from individual planetesimals (Bottke et al., 2005; Rubin and Bottke, 2009). The re-accreation of meteoritic materials to form new parent bodies is well-documented by the complex chondrite breccias (X3-6; X = L, LL, H; see above) or by polymict breccias, which even contain very different chondritic and achondritic ingredients (e.g., Kaidun and Almahata Sitta; e.g., Zolensky et al., 1992; Zolensky and Ivanov, 2003; Bischoff et al., 2010; Goodrich et al., 2014; Horstmann and Bischoff, 2014).

For none of the ordinary chondrite classes a parent body or parent asteroid family has been unequivocally identified, although several such proposals exist (cf., McGraw et al., 2018) and samples of the Hayabusa mission are similar to LL chondrites (e.g., Nakamura et al., 2011). For example, both the asteroid Hebe and members of the Koronis asteroid family have been proposed as sources of H chondrites (Migliorini et al., 1997; Gaffey and Gilbert, 1998; Sanchez et al., 2015). The Koronis family formed some 1-2 Ga ago (Sanchez et al., 2015). On the other hand, Rubin and Bottke (2009) also consider very old source families that might have been around during the heavy cratering epoch 3.7-3.9 Ga ago.

### 4.6.3. Petrologic types require the onion-shell model

The onion-shell configuration of primordial parent bodies (Pellas and Storzer, 1981) is necessary in order to form the chondrites with different degrees of metamorphic overprint (petrologic types 3-6). This was convincingly shown by Trieloff et al. (2003; also considering data of Göpel et al., 1994) for what they considered to be a single original/primordial H chondrite parent body. They demonstrate that the outer shells of the body reached lower maximum metamorphic temperatures and cooled faster than the rocks from the interior. They suggested that the interior needed ~160 Ma to reach 390K. The sizes and detailed formation processes of these bodies may be model dependent.

We definitively need chondritic material that has seen a low degree of (or no) thermal overprint (type 3) and material that has been strongly recrystallized (type 6). Based on their results Trieloff et al. (2003) suggest that the fragmentation and reassembly to trigger the formation of an asteroid with a rubble-pile structure occurred late. Trieloff et al. (2003) do not rule out that similar parent bodies were formed in the same environment. It seems also conceivable that the meteorites studied by these authors derive from more than one – roughly similarly-sized - primordial H chondrite parent body, each having had an onion shell structure.

### 4.6.4. Formation of rubble pile asteroids

The onion-shell model, however, is inconsistent with metallographic cooling rates obtained from Ni-profiles in Fe-rich metal of the three chondrite groups (e.g., Scott and Rajan, 1981, their Fig. 10; Taylor et al., 1987; Bennett and McSween Jr., 1996; Scott et al., 2014). To explain the metallographic data, a disruption of a chondrite parent body, while still hot, combined with rapid re-accretion of the still hot rocky blocks (rubble pile formation) is required (Taylor et al., 1987). Explaining our observations and results of this paper, impacts on a single "giant" onion-shell parent body are clearly necessary to break up the early-formed bodies and may produce mega blocks of the constituents with different degree of recrystallization and equilibration. Such a process is slightly different to the metamorphosed-planetesimal model of Scott and Rajan (1981). These authors suggested that many small (<10 km) planetesimals, in which maximum metamorphic temperatures were reached, existed prior to accretion of the final parent body. Considering both, the Ni-metal cooling rate data and the ages obtained from Pb isotope studies in phosphates, Blackburn et al. (2017) conclude that the large-scale disruption of the H and L chondrite parent bodies happened 60±10 Ma after the formation of CAI (~4505 Ma ago), while earlier (~6 Ma after CAIs) small-scale impact processes may have occurred to explain certain chemical and isotopic characteristics of H4 and L4 chondrites.

Considering the rubble pile formation model, Grimm (1985) and Taylor et al. (1987) proposed nearly complete mixing of chondrite parent bodies by the impact processes mentioned above. This is consistent with our observation in ordinary chondrite breccias in order to place heated material (type 4–6) from the interior of the parent bodies into direct contact with cooler material (type 3) from the outer layers of the body (see also Harrison and Grimm (2010) and Scott et al. (2014)).

### 4.6.5. Three rubble pile asteroids (H, L, LL) or many?

Both the re-accretion of parts of the fragmented "giant" onion-shell like parent body (Grimm, 1985; Taylor et al., 1987) and the accretion of small, metamorphosed planetesimals (Scott and Rajan, 1981) to form a second generation chondrite parent body would result in very similar rubble pile-like objects. As already discussed above, it is unclear whether only three or already many different parent bodies for the ordinary chondrites existed in the early solar system, but it can safely be argued that different breccias of the three chondrite groups originate not only from three single, group-related parent bodies, but from many similar bodies. Since impact processes are witnessed in all kinds of extraterrestrial breccias, no convincing argument exists to believe in single parent bodies for the meteorite groups in general and, in particular, for the ordinary chondrites. As discussed above, Rubin and Bottke (2009) mentioned the probable existence of asteroid families to account for the provenance of H chondrites. This can be supported by simple observations. During an intensive search for CM-like clasts in ordinary chondrites we failed to find one within the thin sections from our collection. However, CM-like clasts are known to exist in some H chondrite breccias (e.g., Abbott, Plainview; Fodor and Keil, 1976, Rubin and Bottke, 2009) and make up several vol% in these chondrite breccias. This may indicate that only distinct members of the H-group asteroid family did have this kind of fragments. In our study we found several CI-like clasts in one H-chondrite but not in others, also supporting the model in favor of the existence of an H-group asteroid family instead of having a single first generation H chondrite parent body. Very similar observations can be made for the LL-group chondrites. Although almost 80% of the meteorites are brecciated and many have clasts of different petrologic types and impact melts, in only one LL3-6 breccia granitic and related achondritic clasts have been identified (Adzhi-Bogdo; Bischoff et al., 1993a; Terada and Bischoff, 2009). The mixing of LL-group chondritic materials with this kind of achondritic material - having oxygen isotope characteristics similar to those of ordinary chondrite - must have been a process restricted to very distinct members of the LL group family.

### 4.6.6. Breccia formation and noble gases

Another argument comes from the characteristics of the L chondrites. As stated above about two thirds of the L chondrites have lost noble gases. This most likely means that about 470 Ma ago one parent body was heavily affected by impact, fragmented (catastrophic fragmentation; Heymann, 1967), and is delivering L chondrite meteorites since that break-up, whereas other meteorites derive from other similar parent bodies of the "L-group family" that did not lose gases in their evolution. In this respect, for NWA 869 (L3-6) different impact events are recorded by an IMR clast at 1790 ± 36 Ma and a shock-darkened clast at 2216 ± 40 Ma, demonstrating that NWA 869 escaped major reset in the course of the event at approximately 470 Ma that affected many L chondrites (Metzler et al., 2011). Alternatively, but less plausible in our view, only a portion of the impacted body lost most of the noble gases in the 470 Ma event as suggested by Crabb and Schultz (1981).

Considering the abundances of shock veins in chondrites described in Chapter 3.3. we found that in general the number of ordinary chondrites with shock veins increases with the petrological type. In all chondrite groups the type 6 chondrites have the highest percentage of shock veins. As already stated earlier, if the shock vein-forming impacts would have happened on the original onion shell-like body, most shock veins should be found in rocks of low petrologic types (types 3 and 4), as they exist in outer parts (at the surface) of the meteorite parent body. Since this is not the case, parent bodies are required that allowed the formation of shock veins (or planes in three dimensions) in highly thermally modified rocks at or near the surface of the parent body. Consequently, the formation of complex ruble-pile-like bodies is certainly needed in order to explain the observations shown and discussed above.

### 4.6.7. Collisions within the last 500 Ma

We do not safely know when the formation of the complex bodies discussed above occurred and how many of these objects formed. However, at least for the L chondrites we can assume that already about 470 Ma ago several parent bodies existed (e.g., Heymann, 1967; Haack et al., 1996). From the determination of the cosmic-ray exposure ages we know that at least one of the H-group parent bodies was catastrophically hit 7 Ma ago. This or perhaps other bodies were already impacted 33 Ma and 24 Ma ago, delivering H chondritic materials to Earth up to today. Considering the L chondrites, major impacts on the parent bodies occurred at 40 and 28 Ma ago. The relative proportions of $^{40}$Ar-poor meteorites and those with normal $^{40}$Ar in these peaks are markedly different, the 28 Ma peak is dominated by poor $^{40}$Ar retainers (Marti and Graf, 1992). A smaller

peak at 5 Ma is only seen in $^{40}$Ar-poor meteorites. This suggests major collisions 28 Ma and 5 Ma ago on an L chondrite parent body which earlier - most likely 470 Ma ago - had suffered catastrophic outgassing (Marti and Graf, 1992), whereas the meteorites with normal $^{40}$Ar likely derive from a different L chondrite parent. It seems unclear whether the more modest fractions of $^{40}$Ar-poor meteorites with exposure ages around 40 Ma as well as the 28 Ma meteorites with a full $^{40}$Ar complement are related to the same collisions (possibly between the two mentioned L-chondrite parent bodies?) or represent a "background population", possibly involving further last generation L chondrite parent bodies. In this respect Keil et al. (1994) also concluded that the 5, 28, and 40 Ma impact events that delivered meteoroids may not all have occurred on the same but perhaps on different fragments that were generated in the 470 Ma catastrophic event. Here, we also suggest that even other L chondrite-related parent bodies may have existed independent from the object that suffered gas-loss 470 Ma ago.

The LL chondrites have exposure ages close to 15 Ma and smaller clusters at 28 Ma and 40 Ma. As already stated above, the latter clusters coincide with those of the L chondrites and may indicate major collisional events in the asteroid belt. The mixing of L and LL chondritic material is well-documented. In many cases L chondrite fragments were encountered in LL chondrite breccias. Examples are Paragould, Glanerbrug, Adzhi-Bogdo, and NWA 5764 (Fodor and Keil, 1978, Bischoff et al., 1993c; Niemeier and Bischoff, 2006; Gattacceca et al., 2017). Gattacceca et al. (2017) showed, that the cosmic-ray exposure ages of the L clast and the LL host chondrite are identical (36.6 ± 5.8 Ma) lying in the 40 Ma cluster. However, it should be mentioned that in general mixing of clasts from different ordinary chondrite groups are rare (for details see Bischoff et al., 2006).

If we consider the distribution of the exposure ages with the distinct peaks, we have to realize that not too many impacts have occurred in order to explain the flux of ordinary chondrite meteoroids to Earth. However, this certainly does not tell anything about the number of "last-generation" parent bodies that exist in the asteroid belt. S asteroids, which are probably made of ordinary chondrite material, are the most abundant type of asteroid in the inner main belt (Burbine et al., 2002).

## 5. CONCLUDING REMARKS

This paper presents the largest data set ever published on brecciation features of a large number of ordinary chondrites. Oxygen isotope data obtained by ion probe demonstrate that some of the most primitive ordinary chondrites contain very different xenolithic fragments. As indicated in Chapter

4.6.1 and since we know that some meteorite parent bodies differentiated 1-2 Ma earlier than the chondrules formed (Kleine et al., 2005, 2008), we have to consider that fragments of early-formed planetary materials (at a time of heavy impact activities) were able to become incorporated into the chondrule formation areas and/or into the subsequent chondrite accretion locations. These suggestions are supported by the occurrence of different xenoliths in type 3 chondrites (compare Fig. 5). That certain chondritic meteorites could represent samples of "second-generation parent bodies" has been discussed earlier (e.g., Sokol et al., 2007 and references therein). Also, Libourel and Krot (2007) considered the presence of metamorphosed planetesimal material among the precursors during formation of magnesian chondrules. These results clearly indicate that the so-called primitive and pristine, type 3 unequilibrated ordinary chondrites are not primitive, but a mixture of early-formed achondritic and chondritic clasts and chondrules. Thus, other meteorite parent bodies (or parts of these) must be considered as precursor parent bodies that delivered materials (e.g., clasts; and these may also include the relict grains in subsequently-formed chondrules) to be involved in chondrule formation or to be ingredients in the mixture of components available for ordinary chondrite parent body accretion about 2 Ma after the formation of CAIs.

This study also includes the aspect of noble gases (presence and abundance) into the discussion on the evolution of the brecciation processes of the studied 2280 ordinary chondrites. Brecciation aspects should be very informative for all cosmochemists, who are studying chemical aspects on bulk meteorites. Textural details are often barely considered in meteorite analysis. This paper emphasizes the importance of these details.

**ACKNOWLEDGEMENTS**

We thank U. Heitmann and Kerstin Klemm (Münster) for technical assistance and the Heidelberg Ion Probe Team (T. Ludwig, M. Trieloff, and A. Schmitt) for the support during the O-isotope analyses of phases in three xenolithic fragments from ordinary chondrites. We thank Thomas Graf for providing his evaluated cosmic ray exposure ages of L chondrites. We also appreciate the very helpful comments and suggestions by Associate Editor R. Jones as well as by A. Ruzicka and two further anonymous reviewers. This work was partly supported by the German Research Foundation (DFG) within the SFB-TRR 170 "Late Accretion onto Terrestrial Planets" (subproject B5). This is TRR 170 publication No. 48.

**REFERENCES**

Agee M.A., Habermann M. A., and Ziegler K. (2018).. Northwest Africa 11575: Unique ungrouped trachyandesite achondrite. *49th Lunar and Planetary Science Conference*. #2226.

Amelin Y., Kaltenbach A., Iizuka T., Stirling C.H., Ireland T.R., Petaev M., and Jacobsen S.B. (2010) U-Pb chronology of the Solar System's oldest solids with variable $^{238}U/^{235}U$. *Earth and Planetary Science Letters* **300**, 343-350.

Anders E. (1964) Origin, age, and composition of meteorites. *Space Science Rev*. **3**, 583-714.

Anders E. (1978) Most stony meteorites come from the asteroid belt, In: *Asteroids: An exploration assessment*, ed. D. Morison, W. C. Wells NASA Conf. Pub. 2053, pp. 57-76.

Bennett M.E. and McSween H. Y. 1996. Revised model calculations for the thermal histories of ordinary chondrite parent bodies. *Meteoritics & Planetary Science* 31:783-792.

Binns R.A. (1967) Structure and evolution of noncarbonaceous chondritic meteorites. *Earth and Planetary Science Letters* **2**, 23-28.

Bischoff A. (1998) Aqueous alteration of carbonaceous chondrites: Evidence for preaccretionary alteration-A review. *Meteoritics & Planetary Science* **33**, 1113-1122.

Bischoff A. and Geiger T. (1995) Meteorites from the Sahara: Find locations, shock classification, degree of weathering, and pairing. *Meteoritics* **30**, 113-122.

Bischoff A. and Schultz L. (2004) Abundance and meaning of regolith breccias among meteorites. *Meteoritics & Planetary Science* **39**, A15.

Bischoff A. and Stöffler D. (1992) Shock metamorphism as a fundamental process in the evolution of planetary bodies: Information from meteorites. *European Journal of Mineralogy* **4**, 707-755.

Bischoff A., Rubin A. E., Keil K., and Stöffler D. (1983) Lithification of gas-rich chondrite regolith breccias by grain boundary and localized shock melting. *Earth and Planetary Science Letters* **66**, 1-10.

Bischoff A., Geiger T., Palme H., Spettel B., Schultz L., Scherer P., Schlüter J., and Lkhamsuren J. (1993a) Mineralogy, chemistry, and noble gas contents of Adzhi-Bogdo – an LL3-6 chondritic breccia with L-chondritic and granitoidal clasts. *Meteoritics* **28**, 570-578.

Bischoff A., Palme H., Schultz L., Weber D., Weber H. W., and Spettel B. (1993b) Acfer 182 and paired samples, an iron-rich carbonaceous chondrite: Similarities with ALH 85085 and relationship to CR chondrites. *Geochimica et Cosmochimica Acta* **57**, 2631-2648.

Bischoff A., Palme H., Ash R.D., Clayton R.N., Schultz L., Herpers U., Stöffler D., Grady M.M., Pillinger C.T., Spettel B., Weber H., Grund T., Endreß M., and Weber D. (1993c) Paired Renazzo-type (CR) carbonaceous chondrites from the Sahara. *Geochim. Cosmochim. Acta* **57**, 1587-1603

Bischoff A., Gerel O., Buchwald V.F., Spettel B., Loeken T., Schultz L., Weber H. W., Schlüter J., Baljinnyam L., Borchuluun D., Byambaa C., and Garamjav D. (1996) Meteorites from Mongolia. *Meteoritics & Planetary Science* **31**, 152-157.

Bischoff A., Weber D., Spettel B., Clayton R. N., Mayeda T. K., Wolf D., and Palme H. (1997) Hammadah al Hamra 180: A unique unequilibrated chondrite with affinities to LL-group ordinary chondrites. *Meteoritics & Planetary Science* **32**, A14.

Bischoff A., Scott E. R. D., Metzler K., and Goodrich C. A. (2006) Nature and origins of meteoritic breccias. In *Meteorites and the Early Solar System II*, edited by Lauretta D.S. and. McSween Jr H.Y. Tucson. University of Arizona. pp. 679-712.

Bischoff A., Horstmann M., Pack A., Laubenstein M., and Haberer S. (2010) Asteroid 2008 $TC_3$ - Almahata Sitta: A spectacular breccia containing many different ureilitic and chondritic lithologies. *Meteoritics & Planetary Science* **45**, 1638–1656.

Bischoff A., Horstmann M., Heusser G., Pack A., and Albrecht N. (2012) Almahata Sitta sample MS-181: The first carbonaceous chondrite ($CB_a$) from Asteroid 2008 $TC_3$. *Meteoritics & Planetary Science* **47**, A71.

Bischoff A., Dyl K. A., Horstmann M., Ziegler K., Wimmer K., and Young E. D. (2013a) Reclassification of Villalbeto de la Peña – occurrence of a winonaite-related fragment in a hydrothermally metamorphosed polymict L-chondritic breccias. *Meteoritics & Planetary Science* **48**, 628-640.

Bischoff A., Horstmann M., Vollmer C., Heitmann U., and Decker S. (2013b) Chelyabinsk – not only another ordinary LL5 chondrite, but a spectacular chondrite breccia (#5171). *Meteoritics & Planetary Science* **48**, A61.

Bischoff A., Horstmann M., Barrat J.-A., Chaussidon M., Pack A., Herwartz D., Ward D., Vollmer C., and Decker S. (2014) Trachyandesitic volcanism in the early Solar System. *Proceedings of the National Academy of Sciences* **111**, 12689-12692.

Bischoff A., Ebert S., Patzek M., Horstmann M., Pack A., Barrat J.-A., and Decker S. (2015) New individuals from the Almahata Sitta strewn field: Old friends and brand-new fellows. *Meteoritics & Planetary Science* **50**, #5092.

Bischoff A., Ebert S., Patzek M., Horstmann M., Pack A., and Decker S. (2016) Almahata Sitta news: Well-known varieties and new species in the zoo (#6319). *Meteoritics & Planetary Science* **51**, A167.

Bischoff A., Barrat J.-A., Bauer K., Burkhardt C., Busemann H., Ebert S., Gonsior M., Hakenmüller J.,Haloda J., Harries D., Heinlein D., Hiesinger H., Hochleitner R., Hoffmann V., Kaliwoda M., Laubenstein M., Maden C., Meier M. M. M., Morlok A., Pack A., Ruf A.,

Schmitt-Kopplin P., Schönbächler M., Steele R. C. J., Spurny P., and Wimmer K. (2017) The Stubenberg meteorite - an LL6 chondrite fragmental breccia recovered soon after precise prediction of the strewn field. *Meteoritics & Planetary Science* **52**, 1683-1703.

Blackburn T., Alexander C.M.O`D., Carlson R., and Elkins-Tanton L. T. (2017) The accretion and impact history of the ordinary chondrite parent bodies. *Geochimica et Cosmochimica Acta* **200**, 201-217.

Bogard D. D. (1995). Impact ages of meteorites: A synthesis. *Meteoritics* **30**, 244-268.

Bogard D. D., Garrison D. H., Norman M., Scott E. R. D., and Keil K. (1995) $^{39}$Ar-$^{40}$Ar age and petrology of Chico: Large scale impact melting on the L chondrite parent body. *Geochimica et Cosmochimica Acta* **59**, 1383-1399.

Bottke W. F., Durda D., Nesvorny D., Jedicke R., Morbidelli A., Vokrouhlicky D., and Levison H. (2005) The origin and evolution of stony meteorites. In *Dynamics of populations of planetary systems*, edited by Knezevic Z. and Milani A. IAU Colloquium **197**, 357-374.

Bridges J. C. and Hutchison R. (1997) A survey of clasts and chondrules in ordinary chondrites. *Meteoritics & Planetary Science* **32**, 389-394.

Bridges J. C., Franchi I. A., Hutchison R., Morse A. D. Long J. V. P., and Pillinger C. T. (1995) Cristobalite- and tridymite-bearing clasts in Parnallee (LL3) and Farmington (L5). *Meteoritics* **30**, 715-727.

Burbine T. H., McCoy T.J., Meibom A., Gladman B., Keil K. (2002) Meteoritic parent bodies: Their number and Identification. In *Asteroids III*, (W. Bottke, A. Cellino, P. Paolicchoi, and R. P. Binzel, eds.), University of Arizona Press, Tucson, 653-667.

Burbine T. H., Folco L., Capitani G., Bland P. A., Menvies O. N., and McCoy T.J. (2003) Identification of nanophase iron in a H chondrite impact melt. *Meteoritics & Planetary Science* **38**, A111.

Casanova I., Keil K., Wieler R., San Miguel A., and King E. A. (1990) Origin and history of chondrite regolith, fragmental and impact-melt breccias from Spain. *Meteoritics* **25**, 127-135.

Chen J. H. and Wasserburg G. J. (1981) The isotopic composition of uranium and lead in Allende inclusions and meteoritic phosphates. *Earth and Planetary Science Letters* **5**, 1445-1456.

Christophe Michel-Lévy M. (1988) A new component of the Mezö-Madaras breccia: A microchondrule- and carbon-bearing L-related chondrite. *Meteoritics* **23**, 45-48.

Connelly J.N., Bizzarro M., Krot A.N., Nordlund Å., Wielandt D., and Ivanova M.A. (2012) The absolute chronology and thermal processing of solids in the solar protoplanetary disk. *Science* **338,** 651-655.

Crabb J. and Schultz L. (1981) Cosmic-ray exposure ages of the ordinary chondrites and their significance for parent body stratigraphy. *Geochimica et Cosmochimica Acta* **45**, 2151-2160.

Dalcher N., Caffee M. W., Nishiizumi K., Welten K. C., Vogel N., Wieler R., and Leya, I. (2013) Calibration of cosmogenic noble gas production in ordinary chondrites based on $^{36}$Cl-$^{36}$Ar ages. Part 1: Refined produced rates for cosmogenic $^{21}$Ne and $^{38}$Ar. *Meteoritics & Planetary Science* **48**, 1841-1862.

Davidson T. M., O`Brien D. P., Ciesla F. J., and Collins G. S. (2013) The early impact histories of meteorite parent bodies. *Meteoritics & Planetary Science* **48**, 1894–1918.

Davis D. R. and Chapman C. R. (1977) The collisional evolution of asteroid composition classes. *Lunar and Planetary Science Conference* **VIII**, 224-226.

Dodd R. T. (1974) Petrology of the St. Mesmin chondrite. *Contributions to Mineralogy and. Petrolology* **46**, 129-145.

Dyl K. A., Bischoff A., Ziegler K., Young E. D. Wimmer K., and Bland P. A. (2012) Early Solar System hydrothermal activity in chondritic asteroids on 1-10-year timescales. *Proceedings of the National Academy of Sciences* **109**, 18306-18311.

Ebert S., Render J., Brennecka G. A., Bischoff A., Burkhardt C., and Kleine T. (2017) $^{50}$Ti excesses in CAIs from ordinary and Rumuruti chondrites. *Meteoritics & Planetary Science* **52**, A78, #6250.

Endress M., Keil K., Bischoff A., Spettel B., Clayton R. N., and Mayeda T. K. (1994) Origin of dark clasts in the Acfer 059/El Djouf 001 CR2 chondrite. *Meteoritics* **29**, 26-40.

Fioretti A. M., Goodrich C. A., Shaddad M., Jenniskens P., Zolensky M., Kohl I., Young E., Rumble D., Kita N., Turrin B., and Herzog G. (2017) A report on 63 newly sampled stones of the Almahata Sitta fall (Asteroid 2008 TC3) from the University of Khartoum Collection, including a C2 carbonaceous chondrite (#1846). *48th Lunar and Planetary Science Conference*. CD-ROM.

Fodor R. V. and Keil K. (1975) Implications of poikilitic textures in LL-group chondrites. *Meteoritics* **10**, 325-340.

Fodor R. V. and Keil K. (1976) Carbonaceous and non-carbonaceous lithic fragments in the Plainview, Texas, chondrite: origin and history. *Geochimica et Cosmochimica Acta* **40**, 177-189.

Fodor R. V., and Keil K., (1978) Catalog of lithic fragments in LL-group chondrites. Special Publication No. 19. University of New Mexico, Institute of Meteoritics, 38 pp.

Folco L., Bland P. A., D`Orazio M., Franchi I. A., and Rocchi S. (2002) Dar al Gani 896: A unique picritic achondrite. *Meteoritics & Planetary Science* **37**, A49.

Funk C., Bischoff A., and Schlüter J. (2011) Xenoliths in carbonaceous and ordinary chondrites. *Meteoritics & Planetary Science* **46**, A71.

Gaffey M. J. and Gilbert S. L. (1998) Asteroid 6 Hebe: The probable parent body of the H-type ordinary chondrites and the IIE iron meteorites. *Meteoritics & Planetary Science* **33**, 1281-1295.

Gattacceca J., Krzesińska A. M., Marrocchi Y., Meier M. M. M., Bourot-Denise M., and Lenssen R. (2017) Young asteroid mixing revealed in ordinary chondrites: The case of NWA 5764, a polymict LL breccia with L clasts. *Meteoritics & Planetary Science* **52**, 2289–2304.

Göpel C., Manhes G., and Allegre C. J. (1994) U-Pb systematics of phosphates from equilibrated ordinary chondrites. *Earth and Planetary Science Letters* **121**, 153-171.

Goodrich C. A., Bischoff A., and O'Brien D. P. (2014) Asteroid 2008 $TC_3$ and the fall of Almahata Sitta, a unique meteorite breccia. *Elements* **10**, 31-37.

Graf T. and Marti K. (1994) Collisional records in LL-chondrites. *Meteoritics* **29**, 643–648.

Graf T. and Marti. K. (1995) Collisional history of H chondrites. *Journal of Geophysical Research: Planets* **100**, 21247–21263.

Grimm R. E. (1985) Penecontemporaneous metamorphism, fragmentation, and reassembly of ordinary chondrite parent bodies. . *Journal of Geophysical Research:* **90**, 2022–2028.

Grossman J. N. and Brearley A. J. (2005) The onset of metamorphism in ordinary and carbonaceous chondrites. *Meteoritics & Planetary Science* **40**, 7-122.

Haack H., Farinella P., Scott E. R. D., and Keil K. (1996) Meteoritic, asteroidal, and theoretical constraints on the 500 Ma disruption of the L chondrite parent body. *Icarus* **119**, 182-191.

Harrison K. P. and Grimm R. E. 2010. Thermal constraints on the early history of the H-chondrite parent body reconsidered. *Geochimica et Cosmochimica Acta* 74:5410-5423.

Herzog G. F. and Caffee M. W. (2014) Cosmic-ray exposure ages of meteorites. In *Treatise in Geochemistry*, 2nd edition, edited by Davis A. M. Oxford: Elsevier. pp. 419–454.

Heymann D. (1967) On the origin of hypersthene chondrites: Ages and shock effects in black chondrites. *Icarus* **6**, 189-221.

Hezel D. (2003) Die Bildung $SiO_2$-reicher Phasen im frühen Sonnensystem. Ph. D. Thesis, Universität zu Köln, pp. 131.

Hirayama K. (1918) Groups of asteroids probably of common origin. *Astronomical Journal* **31**, 185-188.

Horstmann M. and Bischoff A. (2014) The Almahata Sitta polymict breccia and the late accretion of Asteroid 2008 $TC_3$ - Invited Review. *Chemie der Erde - Geochemistry* **74**, 149-184.

Horstmann M., Bischoff A., Pack A., and Laubenstein M. (2010) Almahata Sitta—fragment MS-CH: Characterization of a new chondrite type. *Meteoritics & Planetary Science* **45**, 1657-1667.

Horstmann M., Humayun M., and Bischoff A. (2014) Clues to the origin of metal in Almahata Sitta EL and EH chondrites and implications for primitive E chondrite thermal histories. *Geochimica et Cosmochimica Acta* **140**, 720-744.

Hutchison R. (1996) Chondrules and their associates in ordinary chondrites: A planetary connection. In "*Chondrules and the Protoplanetary Disk"* (eds. R.H. Hewins, R.H. Jones, E.R.D. Scott), 311-318, Cambridge Univ. Press.

Hutchison R., Williams C. T., Din V.K., Clayton R. N., Kirschbaum C., Paul R. L., and Lipschutz M. E. (1988) A planetary, H-group pebble in the Barwell, L6, unshocked chondritic meteorite. *Earth and Planetary Science Letters* **90**, 105-118.

Ivanov A. V. (1989) The Kaidun meteorite: composition and history. *Geochemistry International* **26**, 84-91.

Keil K. (1982) Composition and origin of chondritic breccias. In *Workshop on Lunar Breccias and Soils and Their meteoritic Analogs* (eds. G. J. Taylor and L. L. Wilkening), pp. 65-83. LPI Technical Report 82-02. Lunar and Planetary Institute.

Keil K., Fodor R. V., Starzyk P. M., Schitt R. A., Bogard D. D., and Husain L. (1980) A 3.6-b.y.-old impact melt rock fragment in the Plainview chondrite: Implications for the age of the H-group chondrite parent body regolith formation. *Earth and Planetary Science Letters* **51**, 135-247.

Keil K., Haack H., Scott E. R. D. (1994) Catastrophic fragmentation of asteroids: Evidence from meteorites. *Planetary Space Science* **42**, 1109-1122.

Keil K., Zucolotto M. E., Krot A. N., Doyle P. M., Telus M., Krot T. V., et al. (2015) The Vicencia meteorite fall: A new unshocked (S1) weakly metamorphosed (3.2) LL chondrite. *Meteoritics & Planetary Science* **50**, 1089-1111.

Kennedy A. K., Hutchison R., Hutcheon I. D., and Agrell S. O. (1992) A unique high Mn/Fe microgabbro in the Parnallee (LL3) ordinary chondrite: Nebular micture or planetary differentiate form a previously unrecognized planetary body? *Earth and Planetary Science Letters.* **113**, 191-205.

Kieffer S. W. (1975) From regolith to rock by shock. *The Moon* **13**, 301-320

Kita N. T., Huss G. R., Tachibana S., Amelin Y., Nyquist L. E., and Hutcheon I. D. (2005) Constraints on the origin of chondrules and CAIs from short-lived and long-lived radionuclides. In *Chondrites and the protoplanetary disk*, edited by Krot A. N., Scott E. R. D., and Reipurth B. ASP Conference Series, vol. 341. San Francisco, California: Astronomical Society of the Pacific, 558–587.

Kleine T., Mezger K., Münker C., Palme H., and Bischoff A. (2004) $^{182}$Hf-$^{182}$W isotope systematics of chondrites, eucrites, and martian meteorites: Chronology of core formation and early mantle differentiation in Vesta and Mars. *Geochimica et Cosmochimica Acta* 68: 2935-2946.

Kleine T., Mezger K., Palme H., Scherer E., and Münker C. (2005) Early core formation in asteroids and late accretion of chondrite parent bodies: Evidence from Hf-182-W-182 in CAIs, metal-rich chondrites, and iron meteorites. *Geochimica et Cosmochimica Acta* **69**, 5805-5818.

Kleine T., Touboul M., Van Orman J. A., Bourdon B., Maden C., Mezger K., and Halliday A. N. (2008) Hf-W thermochronometry: Closure temperature and constraints on the accretion and cooling history of the H chondrite parent body. *Earth and Planetary Science Letters* **270**, 106-118.

Korochantseva E. V., Trieloff M., Lorenz C. A., Buykin A. I., Ivanova M. A., Schwarz W. H., Hopp J., and Jessberger E. K. (2007) L-chondrite asteroid breakup tied to Ordovician meteorite shower by multiple isochron Ar-40-Ar-39 dating. *Meteoritics & Planetary Science* **42**, 113-130.

Kracher A., Keil K., and Scott E. R. D. (1982) Leoville (CV3) – An "accretionary breccia"? *Meteoritics* **17**, 239.

Kring D. A., Hill D. H., Gleason J. D., Britt D. T., Consolmagno G. J., Farmer M., Wilson S., and Haag R. (1999) Portales Valley: A meteoritic sample of the brecciated and metal-veined floor of an impact crater on an H-chondrite asteroid. *Meteoritics & Planetary Science* **34**, 663-669.

Libourel G. and Krot A. N. (2007) Evidence for the presence of planetesimal material among the precursors of magnesian chondrules of nebular origin. *Earth and Planetary Science Letters* **254**, 1–8.

MacPherson G. J. (2014) Calcium-aluminum-rich inclusions in chondritic meteorites. In *Treaties on Geochemistry* 2. (ed. A. M. Davis, H. D. Holland, K. K. Turekian). Amsterdam, Netherlands: pp. 139-179.

MacPherson G. J., Jarosewich E., and Lowenstein P. (1993) Magombedze: A new H-chondrite with light-dark structure. *Meteoritics* **28**, 138-142.

Marti K. and Graf T. (1992) Cosmic-ray exposure history of ordinary chondrites. *Annual Review of Earth and Planetary Sciences* **20**, 221-243.

McGraw A. M., Reddy V., and Sanchez J. A. (2018) Do L chondrites come from the Gefion family? *Monthly Notices of the Royal Astronomical Society*, sty250, https://doi.org/10.1093/mnras/sty250

Metzler K., Bischoff A., Greenwood R. C., Palme H., Gellissen M., Hopp J., Franchi I. A., and Trieloff M. (2011) The L3-6 chondritic regolith breccia Northwest Africa (NWA) 869: (I) Petrology, chemistry, oxygen isotopes, and Ar-Ar age determinations. *Meteoritics & Planetary Science* **46**, 652-680.

Migliorini F., Manara A., Scaltriti F., Farinella P., Cellino A., and DiMartino M. (1997). Surface properties of (6) Hebe: A possible parent body of ordinary chondrites. *Icarus* **128**, 104-113.

Misawa K., Watanabe S., Kitamura M., Nakamura N., Yamamoto K., and Masuda A. (1992) A noritic clast from the Hedjaz chondritic breccia: Implications for melting events in the early solar system. *Geochemical Journal* **26**, 435-446.

Mittlefehldt D. W. (1994) The genesis of diogenites and HED parent body petrogenesis. *Geochimica et Cosmochimica Acta* **58**, 1537-1552.

Mittlefehldt D. W. and Lindstrom M. M. (2001) Petrology and geochemistry of Patuxent Range 91501, a clast-poor impact melt from the L chondrite parent body and Lewis Cliff 88663, an L7 chondrite. *Meteoritics & Planetary Science* **36**, 439-457.

Mittlefehldt D. W., Lindstrom M. M., Wang M.-S., and Lipschutz M. E. (1995) Geochemistry and Origin of achondritic inclusions in Yamato-75097, -793241 and-794046 chondrites. *Proceedings of the 8th Symposium on Antarctic Meteorites.* pp. 251-271.

Morlok A., Bischoff A., Patzek M., Sohn M., and Hiesinger H. (2017) Chelyabinsk – a rock with many different (stony) faces: An infrared study. *Icarus* **284**, 431-442.

Nagao K. (1994) Noble gases in hosts and inclusions from Yamato-75097 (L6), -793241 (L6) and –794046 (H5). *Proceedings of the 7th Symposium on Antarctic Meteorites.* pp. 197-216.

Nakamura N., Misawa K., Kitamura M., Masuda A., Watanabe S., and Yamamoto K. (1990a) Highly fractionated REE in the Hedjaz (L) chondrite: Implications for nebular and planetary processes. *Earth and Planetary Science Letters* **99**, 290-302.

Nakamura N., Fujiwara T., and Nofda S. (1990b) Young asteroid melting event indicated by Rb-Sr dating of Point of Rocks meteorite. *Nature* **345**, 51-53.

Nakamura T., Noguchi T., Tanaka M., Zolensky M. E., Kimura M., Tsuchiyama A., Nakato A., Ogami T., Ishida H., Uesugi M., Yada T., Shirai K., Fujimura A., Okazaki R., Sandford S. A., Ishibashi Y., Abe M., Okada T., Ueno M., Mukai T., Yoshikawa M., and Kawaguchi J. (2011) Itokawa dust particles: A direct link between S-type asteroids and ordinary chondrites. *Science* 333, 1113-1116.

Niemeier M. and Bischoff A. (2006) Glanerbrug - an LL4-6 fragmental breccia with huge L chondritic clasts. *Lunar and Planetary Science Conference* **37**, #1625, Lunar and Planetary Institute, Houston.

Norman M. D. and Mittlefehldt D. W. (2002) Impact processing of chondritic planetesimals. Siderophile and volatile element fractionation in the Chico L chondrite. *Meteoritics & Planetary Science* **37**, 329-344.

Okano O., Nakamura N., and Nagao K. (1990) Thermal history of the shock-melted Antarctic LL-chondrites from the Yamato-79 collection. *Geochimica et Cosmochimica Acta* **54**, 3509-3523.

Patzek M. and Bischoff A. (2015) Search and characterization of volatile-rich clasts in brecciated meteorites. *Meteoritics & Planetary Science* **50**, #5057.

Patzek M., Ebert S., and Bischoff A. (2016) New volatile-rich clasts from brecciated chondrites and achondrites (#6136). *Meteoritics & Planetary Science* **51**, A511.

Patzek M., Hoppe P., Bischoff A., Visser R., and John T. (2017) Water-bearing, volatile-rich clasts in howardites and polymict ureilites – carriers of Deuterium-enriched waters not sampled by individual meteorites. *Meteoritics & Planetary Science* **52**, A267, #6183.

Patzek M., Bischoff A., Visser R., and John T. (2018) Mineralogy of volatile-rich clasts in brecciated meteorites. *Meteoritics & Planetary Science* (accepted, in press).

Pellas P. and Storzer D. (1981) $^{244}$Pu fission track thermometry and its application to stony meteorites. *Proc. Royal Soc. London*, Ser. **A 374**, 253–270.

Prinz M., Nehru C. E., Weisberg M. K., Delany J. S., Yanai K., and Kojima H. (1984) H-chondritic clasts in a Yamato L6 chondrite: Implications for metamorphism. *Meteoritics* **19**, 292-293.

Raack J. (2007) Der Meteorit Ramsdorf – Geschichtliche Aspekte und mineralogische Untersuchungen. Bachelor Thesis. Institut für Planetologie, Universität Münster, 1-83.

Rambaldi E. R. (1981) Relict grains in chondrules. *Nature* **293**, 558–561.

Povinec P. P., Masarik J., Sykora I., Kovacik A., Beno J., Meier M. M. M., Wieler R., Laubenstein M., and Porubcan V. (2015). Cosmogenic radionuclides in the Kosice meteorite: Experimental investigations and Monte Carlo simulations. *Meteoritics & Planetary Science* **50**, 880–892.

Rubin A. E. (1989) An olivine-microchondrule-bearing clast in the Krymka meteorite. *Meteoritics* **24**, 191-192.

Rubin A. E. (1997) The Galim LL/EH polymict breccia: Evidence for impact-induced exchange between reduced and oxidized meteoritic material. *Meteoritics & Planetary Science* **32**, 489-492.

Rubin A. E. (2002) Smyer H-chondrite impact-melt breccia and evidence for sulfur vaporization. *Geochimica et Cosmochimica Acta* **66**, 699-711.

Rubin A.E. and Bottke W. F. (2009) On the origin of shocked and unshocked CM clasts in H-chondrite regolith breccias. *Meteoritics & Planetary Science* **44**, 701–724.

Rubin A. E. and Jones R. H. (2003) Spade: An H chondrite impact-melt breccia that experienced post shock annealing. *Meteoritics & Planetary Science* **38**, 1507-1520.

Rubin A. E. and Moore W. B. (2011) What´s up? Preservation of gravitational direction in the Larkman Nunatak 06299 LL impact melt breccia. *Meteoritics & Planetary Science* **46**, 737-747.

Rubin A. E., Scott E. R. D., and Keil K. (1982) Microchondrule-bearing clast in the Piancaldoli LL3 meteorite: A new kind of type 3 chondrite and its relevance to the history of chondrules. *Geochimica et Cosmochimica Acta* **46**, 1763-1776.

Rubin A. E., Rehfeldt A., Peterson E., Keil K., and Jarosewich E. (1983) Fragmental breccias and the collisional evolution of ordinary chondrite parent bodies. *Meteoritics* **18**, 179-196.

Rubin A. E., Ulff-Moller F., Wasson J. T., and Carlson W. D. (2001) The Portales Valley meteorite breccia: Evidence for impact-induced melting and metamorphism of an ordinary chondrite. *Geochimica et Cosmochimica Acta* **65**, 323-342.

Rubin A. E., Trigo-Rodriguez J. M., Kunihiro T., Kallemeyn G. W., and Wasson J. T. (2005) Carbon-rich chondritic clast PV1 from the Plainview H-chondrite regolith breccia: Formation from H3 chondrite material by possible cometary impact. *Geochimica et Cosmochimica Acta* **69**, 3419–3430.

Ruzicka A., Kring D. A., Hill D. H., Boynton W. V., Clayton R. N., and Mayeda T. K. (1995) Silica-rich orthopyroxenite in the Bovedy chondrite. *Meteoritics* **30**, 57-70.

Ruzicka A., Snyder G. A., and Taylor L. A. (1998) Mega-chondrules and large, igneous-textured clasts in Julesberg (L3) and other ordinary chondrites: Vapor-fractionation, shock-melting, and chondrule formation. *Geochimica et Cosmochimica Acta* **62**, 1419-1442.

Sanchez J. A., Reddy V., Dykhuis M., Lindsay S., and Le Corre L. (2015) Composition of potentially hazardous asteroid (214869) 2007 PA8: An H chondrite from the outer asteroid belt. *The Astrophysical Journal* **808**, 93.

Sanders I. S. (1996) A chondrule-forming scenario involving molten planetesimals. In "*Chondrules and the Protoplanetary Disk"* (eds. R.H. Hewins, R.H. Jones, E.R.D. Scott), 327-334, Cambridge Univ. Press.

Sato G., Takeda H., Yanai K., and Kojima H. (1982) Electron microprobe study of impact-melted regolith breccias (abstract). In *Workshop on Lunar Breccias and Soils and Their meteoritic Analogs* (eds. G. J. Taylor and L. L. Wilkening), pp. 120-122. LPI Technical Report 82-02. Lunar and Planetary Institute.

Schleiting M. (2014) Brekziierung in LL Chondriten. Bachelor Thesis, Institut für Planetologie, WWU Münster, 1-54.

Schleiting M. (2017) Brecciation and shock processes on ordinary chondrite parent bodies. Master Thesis, Institut für Planetologie, WWU Münster, 1-151.

Schleiting M. and Bischoff A. (2015) Brecciation of LL chondrites. *Paneth-Kolloquium*, Nördlingen (Germany), abstract #0015.

Schleiting M. and Bischoff A. (2017) Brecciation of ordinary chondrites - survey of 2248 meteorites. *Meteoritics & Planetary Science* **52**, A306, #6085.

Schultz L. and Franke L. (2004) Helium, neon, aynd argon in meteorites: A data collection. *Meteoritics & Planetary Science* **39**, 1889-1890

Schultz L. and Signer P. (1977) Noble gases in the St: Mesmin chondrite: Implications to the irradiation history of a brecciated meteorite. *Earth and Planetary Science Letters* **36**, 363-371.

Scott E. R. D. (2002) Meteorite evidence for the accretion and collisional evolution of asteroids. In *Asteroids III* (W. Bottke, A. Cellino, P. Paolicchoi, and R. P. Binzel, eds.), University of Arizona Press, Tucson, 697-709.

Scott E. R. D. and Rajan R. S. (1981). Metallic minerals, thermal histories and parent bodies of some xenolithic, ordinary chondrite meteorites. *Geochimica et Cosmochimica Acta* **45**, 53-67.

Scott E. R. D. and Taylor G. J. (1982) Primitive breccias among the type 3 ordinary chondrites – origin and relation to regolith breccias. In *Workshop on Lunar Breccias and Soils and Their*

*meteoritic Analogs* (eds. G. J. Taylor and L. L. Wilkening), pp. 130-134. LPI Technical Report 82-02. Lunar and Planetary Institute.

Scott E. R. D., Taylor G. J., Newsom H., Herbert F., Zolensky M., and Kerridge J. F. (1989) Chemical, themal and impact processing of asteroids. In *Asteroids II*, (R. P. Binzel et al., eds.), University of Arizona Press, Tucson, 701-739.

Scott E. R. D., Krot T. V., Goldstein J. I., Wakita S. (2014) Thermal and impact history of the H chondrite parent asteroid during metamorphism: Constraints from metallic Fe-Ni. *Geochimica et Cosmochimica Acta* **136**, 13-37.

Semenenko V. P., Bischoff A., Weber I., Perron C., and Girich A. L. (2001) Mineralogy of fine-grained material in the Krymka (LL3.1) chondrite. *Meteoritics & Planetary Science* **35**, 1067-1085.

Sepp B., Bischoff A., and Bosbach D. (2001) Low-temperature phase decomposition in iron-nickel metal of the Portales Valley meteorite. *Meteoritics & Planetary Science* **36**, 587-595.

Sokol A. K., Bischoff A., Marhas K. K., Mezger K., and Zinner E. (2007a) Late accretion and lithification of chondritic parent bodies: Mg isotope studies on fragments from primitive chondrites and chondritic breccias. *Meteoritics & Planetary Science* **42**, 1291-1308.

Sokol A. K., Mezger K., Chaussidon M. and Bischoff A. (2007b) Simultaneous accretion of differentiated or metamorphosed asteroidal clasts and chondrules. *Meteoritics & Planetary Science* **42**, A143.

Stöffler D., Bischoff A., Buchwald V. and Rubin A. E. (1988) Shock effects in meteorites. In Kerridge, J.F. & Matthews, M.S. (eds.) *Meteorites and the Early Solar System*: 465-202. The University of Arizona Press. Tucson, AZ.

Stöffler D., Keil K., and Scott E. R. D. (1991) Shock metamorphism of ordinary chondrites. *Geochimica et Cosmochimica Acta* **55**, 3845-3867.

Stöffler D., Hamann C., and Metzler K. (2018) Invited Review – Shock metamorphism of planetary silicate rocks and sediments: Proposal for an updated classification system. *Meteoritics & Planetary Science* **53**, 5-49.

Takeda H., Huston T. J., and Lipschutz M. E. (1984) On the chondrite-achondrite transition: Mineralogy and chemistry of Yamato-74160 (LL7). *Earth and Planetary Science Letters* **71**, 329-339.

Taylor G. J., Keil K., Berkley J. L. and Lance D. E. (1979) The Shaw meteorite: History of a chondrite consisting of impact-melt and metamorphic lithologies. *Geochimica et Cosmochimica Acta* **43**, 323-337.

Taylor G. J., Maggiore P., Scott E. R. D., Rubin A. E., and Keil K. (1987) Original structures and fragmentation and reassembly history of asteroids: Evidence from meteorites. *Icarus* **69**, 1-13.

Terada K. and Bischoff A. (2009) Asteroidal granite-like magmatism 4.53 Gyr ago. *The Astrophysical Journal* **699**, L68-L71.

Trigo-Rodriguez J. M., Llorca J., Weyrauch M., Bischoff A., Moyano-Cambero C. E., Keil K., Laubenstein M., Pack A., Madiedo J. M., Alonso-Azcárate J., Riebe M., Wieler R., Ott U., Tapia M., and Mestres N. (2014) The Ardón L6 ordinary chondrite: A long hidden Spanish meteorite fall. *Meteoritics & Planetary Science* **49**, 1475-1484.

Trieloff M., Jessberger, E. K., Herrwerth I., Hopp J., Fieni C., Ghelis M., Bourot-Denise M., and Pellas P. (2003) Structure and thermal history of the H-chondrite parent asteroid revealed by thermochronometry. *Nature* **422**, 502-506.

Urey H.C. (1959) Primary and secondary objects. *Journal of Geophysical Research* **64**, 1721-1737.

Urey H.C. (1967) Parent bodies of the meteorites and origin of chondrules. *Icarus* **7**, 350-359.

Van Kooten G. K and Buseck P. R. (1978) Interpretation of olivine zoning: Study of a maar from San Francisco volcanic field, Arizona. *Geological Society of America Bulletin* **89**, 744-754.

Vernazza P., Zanda B., Binzel R. P., Hiroi T., DeMeo F. E., Birlan M., Hewins R., Ricci L., Barge P., and Lockhart M. (2014) Multiple and Fast: The accretion of ordinary chondrite parent bodies. *The Astrophysical Journal* **791**, 120.

Vogel N., Wieler R., Bischoff A., and Baur H. (2003) Microdistribution of primordial Ne and Ar in fine-grained rims, matrices, and dark inclusions of unequilibrated chondrites – Clues on nebular processes. *Meteoritics & Planetary Science* **38**, 1399-1418.

Wänke H. (1968) Radiogenic and cosmic ray exposure ages of meteorites, their orbits and parent bodies. In*: The origin and distribution of the elements* (Ed: Ahrens L. H.) 411-421.

Wasson J. T. (1974) Meteorites. *Springer-Verlag*.

Wasson J. T. (1995) Sampling the asteroid belt: How biases make it difficult to establish meteorite-asteroid connections (abstract). *Meteoritics* **30**, 595.

Welten K., Leclerc M. D., Ott U., Metzler K., Caffee M. W., Jull A. J. T., and Franke L. (2011) The L3-6 chondritic regolith breccia Northwest Africa (NWA) 869: (II) Noble gases and cosmogenic radionuclides. *Meteoritics & Planetary Science* **46**, 970-988.

Weyrauch M. and Bischoff A. (2012) Macrochondrules in chondrites – Formation by melting of mega-sized dust aggregates and/or by rapid collisions at high temperatures? *Meteoritics and Planetary Science* **47**, 2237-2250.

Weyrauch M., Horstmann M., and Bischoff A. (2018) Chemical variations of sulfides and metal in enstatite chondrites – Introduction of a new classification scheme. *Meteoritics & Planetary Science* 53 (in press). DOI: 10.1111/maps.1302.

Wieler R. (2002) Cosmic-ray-produced noble gases in meteorites. Noble Gases in Geochemistry and Cosmochemistry. *Reviews in Mineralogy and Geochemistry* **47**, 125–170.

Wieler R., Baur H., Pedroni A., Signer P., and Pellas P. (1989a) Exposure history of the regolithic chondrite Fayetteville: I. Solar-gas-rich matrix. *Geochimica et Cosmochimica Acta* **53**, 1441-1448.

Wieler R., Graf T., Pedroni A., Signer P., Pellas P., Fieni C., Suter M., Vogt S., Clayton R. N., and Laul J. C. (1989b) Exposure history of the regolithic chondrite Fayetteville: II. Solar-gas-free light inclusions. *Geochimica et Cosmochimica Acta* **53**, 1449-1459.

Yamaguchi A., Scott E. R. D., and Keil K. (1998) Origin of unusual impact melt rocks, Yamato-790964 and -790143 (LL chondrites). *Antarctic Meteorite Research* **11**, 18-31.

Yamaguchi A., Scott E. R. D., and Keil K. (1999) Origin of a unique impact-melt rock - The L chondrite Ramsdorf. *Meteoritics & Planetary Science* **34**, 49-59.

Zähringer J. 1968. Rare gases in stony meteorites. *Geochimica et Cosmochimica Acta* 32:209-237.

Zappalà V., Cellino A., Dell'Oro A., Paolicchi P. (2002) Physical and dynamical properties of asteroid families. In *Asteroids III* (W. Bottke, A. Cellino, P. Paolicchoi, and R. P. Binzel, eds.), University of Arizona Press, Tucson, 619-631.

Zolensky M. E. and Ivanov A. (2003) The Kaidun microbreccia meteorite: A harvest from the inner and outer asteroid belt. *Chemie der Erde - Geochemistry* **63**, 185-246.

Zolensky M. E., Hewins R. H., Mittlefehldt D. W., Lindstrom M. M., Xiao X., Lipschutz M. E. (1992) Mineralogy, petrology and geochemistry of carbonaceous chondritic clasts in the LEW 85300 polymict eucrite. *Meteoritics* **27**, 596-604.

Zolensky M. E., Ivanov A. V., Yang S. V., Mittlefehldt D. W., and Ohsumi K. (1996) The Kaidun meteorite: Mineralogy of an unusual CM1 lithology. *Meteoritics & Planetary Science* **31**, 484-493.

Zolensky M., Herrin J., Mikouchi T., Ohsumi K., Friedrich J., Steele A., Rumble D., Fries M., Sandford S., Milam S., Hagiya K., Takeda H., Satake W., Kurihara T., Colbert M., Hanna R., Maisano J., Ketcham R., Goodrich C. A., Le L., Robinson G., Martinez J., Ross K., Jenniskens P. and Shaddad M. H. (2010) Mineralogy and petrography of the Almahata Sitta ureilite. *Meteoritics & Planetary Science* **45**, 1618–1637.

Zook H. A. (1980) A new impact model for the generation of ordinary chondrites. *Meteoritics* **15**, 390-391.

Table 1: Brecciation among 2280 studied ordinary chondrites. Samples in brackets exclude desert chondrites from the dense collection areas Acfer, Dar al Gani, Dhofar, Hammadah al Hamra, NWA, Sahara, Sayh al Uhaymir, and Tanezrouft. *) indicates the occurrence (location) of shock veins within the meteorites. Example: (94/6) = in 94% of the chondrites with shock veins, the veins crosscut the entire meteorite, in 6% of the cases shock veins are restricted to individual fragments. **) 2% are undefined. The data of Scott et al. (1989) are published as "lower limits". See also Table 4, which considers regolith breccias and the number of samples of each petrologic type.

| **Chondrite Group** | **H** | **L** | **LL** |
|---|---|---|---|
| Number of samples | 1193 (216) | 947 (193) | 140 (27) |
| Brecciated chondrites | | | |
| Total number | 276 (46) | 220 (37) | 110 (21) |
| Breccias in % | 23 (21) | 23 (19) | 79 (78) |
| Binns (1967) in % | 33 | 20 | 66 |
| Scott et al. (1989) in % | 24 | 18 | 58 |
| Chondrites with shock veins | | | |
| Total number (all chondrites) | 310 | 377 | 63 |
| Data in % | 26 | 40 | 45 |
| Breccias with shock veins | 133 | 134 | 57 |
| Data in % | 48 | 61 | 52 |
| Location of shock veins in %* | 94/6 | 91/7** | 60/40 |

Table 2: Oxygen isotope composition of olivines and the phyllosilicate-rich matrix in different clasts from the "primitive", type 3 ordinary chondrites Adrar 003 (LL3.1) NWA 5697 (L3), and Sahara 98645 (H3). SIMS-analyses. Compare Figures 5 and 6.

| **Sample** | **Mineral** | **$\delta^{18}O$** | **1σ** | **$\delta^{17}O$** | **1σ** | **$\Delta^{17}O$** | **1σ** |
|---|---|---|---|---|---|---|---|
| NWA 5697 (L3) Graphite-bearing clast | Fo77 | 7.97 | 0.07 | 3.01 | 0.21 | -1.14 | 0.22 |
| NWA 5697 (L3) Graphite-bearing clast | Fo77 | 7.77 | 0.07 | 3.05 | 0.31 | -0.99 | 0.31 |
| NWA 5697 (L3) Graphite-bearing clast | Fo77 | 7.87 | 0.07 | 2.73 | 0.27 | -1.36 | 0.28 |
| NWA 5697 (L3) Graphite-bearing clast | Fo77 | 7.90 | 0.07 | 2.64 | 0.25 | -1.47 | 0.25 |
| | | | | | | | |
| Adrar 003 (LL3.10) Graphite-bearing clast | Fo75 | 8.39 | 0.06 | 3.73 | 0.27 | -0.63 | 0.28 |
| Adrar 003 (LL3.10) Graphite-bearing clast | Fo81 | 8.32 | 0.07 | 3.97 | 0.31 | -0.36 | 0.32 |
| Adrar 003 (LL3.10) Graphite-bearing clast | Fo79 | 7.97 | 0.07 | 3.28 | 0.24 | -0.86 | 0.25 |
| Adrar 003 (LL3.10) Graphite-bearing clast | Fo80 | 8.09 | 0.08 | 3.19 | 0.25 | -1.01 | 0.26 |
| | | | | | | | |
| Sahara 98645 (H3) CI-like clast | Matrix | 16.89 | 0.13 | 10.98 | 0.33 | 2.20 | 0.36 |
| Sahara 98645 (H3) CI-like clast | Matrix | 18.03 | 0.09 | 10.53 | 0.36 | 1.16 | 0.37 |
| Sahara 98645 (H3) CI-like clast | Fo99 | 0.42 | 0.07 | -1.92 | 0.32 | -2.14 | 0.33 |

Table 3: List of brecciated chondrites with impact melt rock clasts and of impact melt breccias (IMB).

| Name | Classification | Name | Classification |
|---|---|---|---|
| **H chondrites** | | | |
| Acfer 022 | H3.7 | Hammadah al Hamra 068 | H5/6 |
| Acfer 171 | H3.7 | Hammadah al Hamra 081 | H6 |
| Acfer 239 | H6 | Hammadah al Hamra 161 | H6 |
| Acfer 259 | H3-6 | Hammadah al Hamra 217 | H4-5 |
| Acfer 301 | H4 | Kosice | H5 |
| Anthony | H5 | Northwest Africa 2443 | H3-5 |
| Chergach | H5 | Northwest Africa 3360 | H3-5 |
| Dar al Gani 043 | H5-6 | Northwest Africa 4211 | H3-6 |
| Dar al Gani 167 | H5-6 | Northwest Africa 4463 | H6 |
| Dar al Gani 241 | H-IMB | Northwest Africa 4582 | H4-6 |
| Dar al Gani 242 | H-IMB | Northwest Africa 2199 | H-IMB |
| Dar al Gani 315 | H3-5 | Northwest Africa 2457 | H-IMB |
| Dhofar 243 | H6 | Northwest Africa 2533 | H-IMB |
| Dhofar 590 | H6 | Sahara 98062 | H4 |
| El Atchane 001 | H3 | Sahara 98100 | H-IMB |
| Gao-Guenie | H5 | Sayh al Uhaymir 075 | H3-5 |
| Hammadah al Hamra 068 | H-IMB | | |
| **L chondrites** | | | |
| Acfer 039 | L3.8 | Northwest Africa 4206 | L3-6 |
| Acfer 069 | L-IMB | Northwest Africa 5068 | L4 |
| Acfer 080 | L3.9 | Northwest Africa 869 | L3-6 |
| Barratta | L4 | Northwest Africa 8262 | L-IMB |
| Catherwood | L-IMB | Sahara 00171 | L-IMB |
| Chico | L6 | Sahara 00194 | L-IMB |
| Dar al Gani 049 | L4/5 | Sahara 00215 | L-IMB |
| Hammadah al Hamra 084 | L6 | Sahara 97057 | L4-6 |
| Hammadah al Hamra 213 | L3-6 | Sahara 98312 | L-IMB |
| Julesburg | L3.6 | Sahara 98782 | L3 |
| Marlow | L5 | Sahara 99362 | L-IMB |
| Motpena (a) | L6 | Sahara 99534 | L5-6 |
| Northwest Africa 1485 | L5-6 | Tsarev | L5 |
| Northwest Africa 3345 | L3-6 | Ramsdorf | L-IMB |
| **LL chondrites** | | | |
| Acfer 091 | LL5-6 | Hammadah al Hamra 181 | LL4-6 |
| Acfer 126 | LL5-6 | Northwest Africa 1489 | LL4-6 |
| Adzhi Bogdo | LL3-6 | Northwest Africa 5078 | LL4-6 |
| Chelyabinsk | LL5-6 | Northwest Africa 3351 | LL-IMB |
| Dar al Gani 061 | LL5-6 | Parambu | LL5-6 |
| Dar al Gani 062 | LL5-6 | | |

Table 4: Fraction of brecciated ordinary chondrites and fraction of regolith breccias (with solar noble gases) among them

| | number of meteorites in Table A1 | number & fraction brecciated | meteorites with noble gas data | brecciated meteorites with noble gas data | meteorites with solar noble gases | fraction of regolith breccias |
|---|---|---|---|---|---|---|
| H3 | 112 | 75 (67%) | 45(40%) | 25(33%) | 16(36%) | 64% |
| H4 | 210 | 44(21%) | 18(8.6%) | 5(11%) | 2(11%) | 40% |
| H5 | 608 | 103(17%) | 49(8.1%) | 7(6.8%) | 5(10%) | 71% |
| H6 | 256 | 47(18%) | 21(8.2%) | 5(11%) | 3(14%) | 60% |
| IMB | 7 | 7(100%) | 0 | 0 | 0 | -- |
| **H total** | **1193** | **276(23%)** | **133(11%)** | **42(15%)** | **26(20%)** | **62%** |
| L3 | 82 | 57(70%) | 9(11%) | 5(8.8%) | 2(22%) | 40% |
| L4 | 80 | 26(33%) | 14(18%) | 3(12%) | 0(0%) | 0 |
| L5 | 206 | 45(22%) | 24(12%) | 10(23%) | 1(4.2%) | 10% |
| L6 | 570 | 83(15%) | 53(9.3%) | 9(11%) | 0 | 0 |
| IMB | 9 | 9(100%) | 0 | 0 | 0 | -- |
| **L total** | **947** | **220(23%)** | **100(11%)** | **27(12%)** | **3(3.0%)** | **11%** |
| LL3 | 22 | 18(82%) | 9(41%) | 8(44%) | 0 | 0 |
| LL4 | 31 | 28(90%) | 9(29%) | 8(29%) | 0 | 0 |
| LL5 | 48 | 34(71%) | 14(29%) | 12(35%) | 2(14%) | 17% |
| LL6 | 38 | 29(76%) | 4(11%) | 3(10%) | 1(25%) | 33% |
| IMB | 1 | 1(100%) | 0 | 0 | 0 | -- |
| **LL Total** | **140** | **110(79%)** | **36(26%)** | **31(28%)** | **3(8.3%)** | **9.7%** |
| **OC total** | **2280** | **605(27%)** | **269(12%)** | **100(17%)** | **32(12%)** | **32%** |

Reading example: 75 of the 112 (=67%) H3 meteorites in Table A1 are brecciated
For 45 of the 112 (= 40%) noble gas data exist
For 25 of the 75 brecciated H3s (33%) noble gas data exist
16 of the 45 (=36%) with noble gas data contain solar noble gases, i. e. are regolith breccias;
64% of all brecciated H3s with noble gas data are regolith breccias (i. e. 16 of 25)
IMB: Impact melt breccias

Classification is as listed in the respective sheets in Table A1 (e. g. H3-6 meteorites are given here as H3)

Table 5: Regolith breccias among the studied chondrites and breccias. *) 26/133 means that from 133 H- chondrites that have been analyzed for noble gases 26 contain solar wind-implanted gases and have to be classified as regolith breccias.

| **Chondrite group** | H | L | LL |
|---|---|---|---|
| Breccias in % (see Table 1) | 23 | 23 | 79 |
| Regolith breccias in % of all meteorites<br>this work | 19.5 (26/133)* | 3.0 (3/100) | 8.3 (3/36) |
| Regolith breccias in % of all meteorites<br>Crabb and Schultz (1981)<br>Graf and Marti (1994, 1995) | <br>14.0<br>14.6 | <br>2.9<br> | <br><br>4.5 |
| Regolith breccias in % of all breccias which were analyzed for noble gases | 62 | 11 | 10 |

## FIGURE CAPTIONS

Fig. 1: Photomicrographs of different areas from the monomict L6 breccia Tenham. a) shock veins are barely visible; b) thick shock veins are clearly visible; c) area, in which the monomict brecciation of Tenham is very obvious. Images in polarized light, crossed Nicols.

Fig. 2: Different individuals with distinct lithologies of the Chelyabinsk LL5-6 breccia: (a) Light-colored, shock-veined LL5/6 lithology; polarized light, crossed Nicols. (b) Brecciated texture of a fragment from the strewn field. The opaque veins and areas between the clasts contain abundant metals and sulfides; image in plane polarized light. (c) Shock-darkened individual in reflected light; metals and sulfides (white veins) fill up the cracks and pores of the silicate-rich rock. (d) Slice of a hand-specimen of an impact melt breccia from the Chelyabinsk strewn field. Some chondrite fragments are embedded in the impact melt. See more details in Bischoff et al. (2013) and Morlok et al. (2017).

Fig. 3: Histograms showing (a) the abundances of brecciated chondrites of the various petrologic types and (b) the abundances of regolith breccias among the studied 2280 ordinary chondrites. See Table 4 for more details.

Fig. 4: (a) LL3-6 polymict meteorite breccia Adzhi-Bogdo (stone) consisting of various types of clasts embedded in a fine-grained matrix. Components of the breccia include chondrules, melt rock clasts, highly-recrystallized rock fragments ("granulites"), breccia clasts, pyroxene-rich fragments with achondritic textures, and alkali-granitoids (Bischoff et al., 1993). (b) L4-6 polymict meteorite breccia NWA 2555. (c) H3-5 chondrite breccia Dar al Gani 300. (d) LL6 monomict meteorite breccia NWA 5074. (e) Light-colored, highly-recrytallized fragment embedded in the clastic matrix of the L3-6 chondrite regolith breccia Adzhi-Bogdo. Images in plane polarized light.

Fig. 5: Xenolithic or highly recrystallized fragments in so-called primitive type 3 ordinary chondrites (a) Krymka (LL3.2): A chondritic fragment occurs as a foreign rock (chondrite in a chondrite). (b) Adrar 003 (LL3.10): A graphite-rich, rounded clast (about 3 mm in size) with a porphyritic olivine-rich texture. Most of the vein-like opaque areas consist of graphite. (c) Adrar 003 (LL3.10): A metamorphosed fragment with a relict barred-olivine chondrule as a rounded object co-existing with typical chondrules. (d) Sahara 98645 (H3): A ~200 µm-sized fragment that is surrounded by chondrules has similarities to CI- chondrites (CI-like clast). Magnetites (mag), calcites (CC), and pyrrhotite (pyrh) are embedded in a phyllosilicate matrix.

Fig. 6: Oxygen isotopic composition of foreign fragments in ordinary chondrites. Data from achondritic clasts from Adzhi-Bogdo (LL3-6) and Study Butte (H3-6) are averages of several analyses from Sokol et al. (2007b). The clast related to winonaites (win) in Villalbeto de la Pena (L6) is from Dyl et al. (2012) and Bischoff et al. (2013). The graphite-bearing clasts from Adrar 003 (LL3.10) and NWA 5697 (L3) have a very similar composition (Table 2) as bulk ureilites and the ALM-A trachyandesite from the Almahata Sitta meteorite strewn field (Bischoff et al., 2014). The phyllosilicates (Phyl) and olivine (Ol) of the CI-like clast in the Sahara 98645 (H3) chondrite cover a wide area (compare Table 2).

Fig. 7: Shock veins in ordinary chondrites: (a) shock veins cutting through the whole meteorites of Villalbeto de la Pena (arrows), Ardon (b; L6 breccias), and fragments of Chelyabinsk (e; LL5-6 breccia). In other cases shock veins are locally limited to individual fragments (c,d from NWA 6381 (LL4-6); f from Adzhi-Bogdo (LL3-6): The shock vein stops abruptly at the edge of the light-colored, highly-metamorphosed fragment (arrow).

Fig. 8: Characteristic features of impact melt areas in ordinary chondrite breccias: (a) Interior of an impact melt breccia clast from NWA 2443 (H3-6) showing abundant zoned newly-formed olivine crystals with Fo rich cores (~$Fa_{7-10}$) surrounded by Fa-rich rims (light grey). In addition fragments of the host lithology (cores with $Fa_{17-18}$) occur as unmelted relicts. Both olivine generations are embedded in a fine-grained to glassy mesostasis. (b) Another impact fragment from NWA 2443 (H3-6), which is greatly equilibrated and its olivines do not show any zoning. This impact fragment has experienced annealing (metamorphism) prior to ejection, mixing and incorporation into the present chondrite breccia. (c) Dar Al Gani 167 (H5-6): Zoned olivines with cores of $Fa_{7-12}$ are

enclosed within a fine-grained groundmass. (d) Impact melt in NWA 3345 (L3-6): Elongated ($Fa_{20-24}$) and blocky olivine ($Fa_{12-16}$) are embedded in a glassy mesostasis. (e) Sahara 97057 (L4-4): Impact melt with zoned olivines having cores of ~$Fa_{17}$. The rims and smaller grains are richer in Fe. (f) Metal-troilite globule within the impact melt fragment of Dar al Gani 167 (H5-6). The metal within the globule is white. Images in back-scattered electrons.

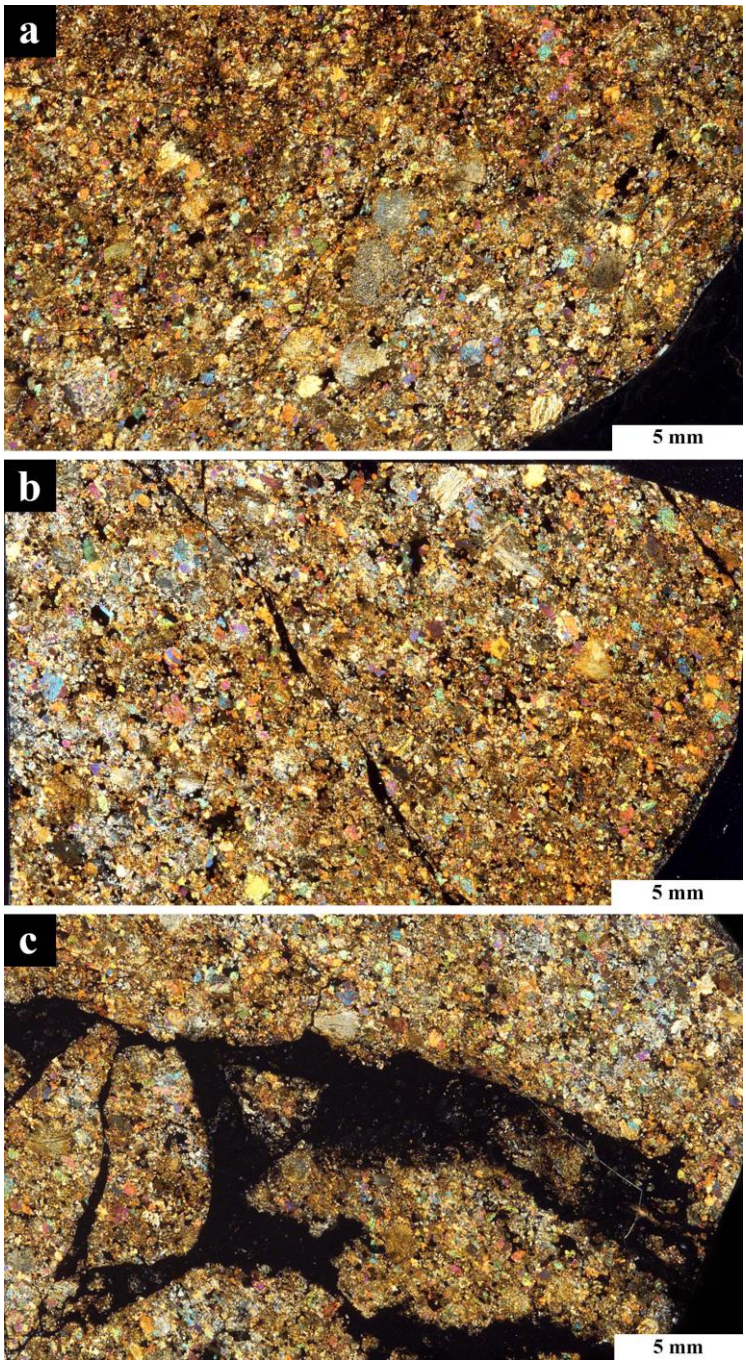


Fig. 1

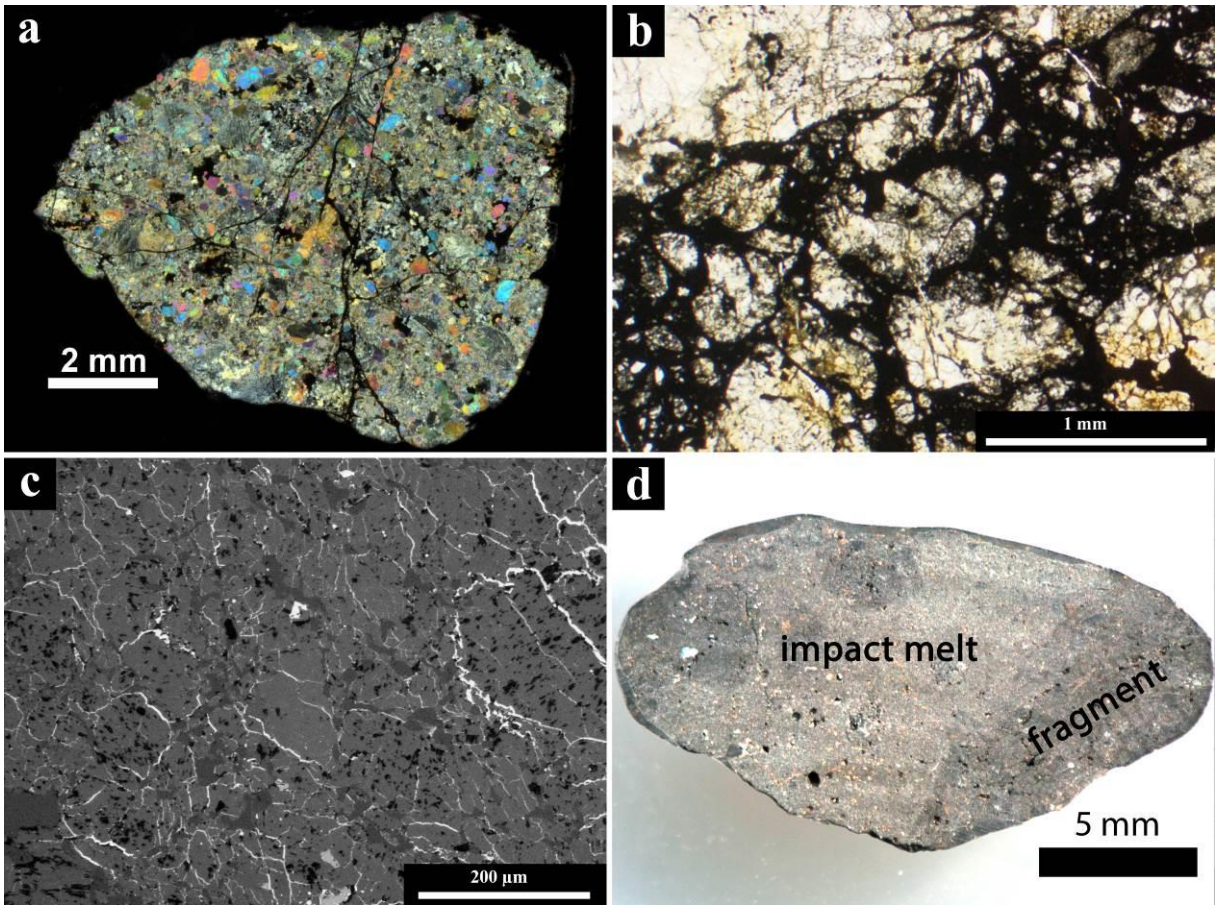


Fig. 2

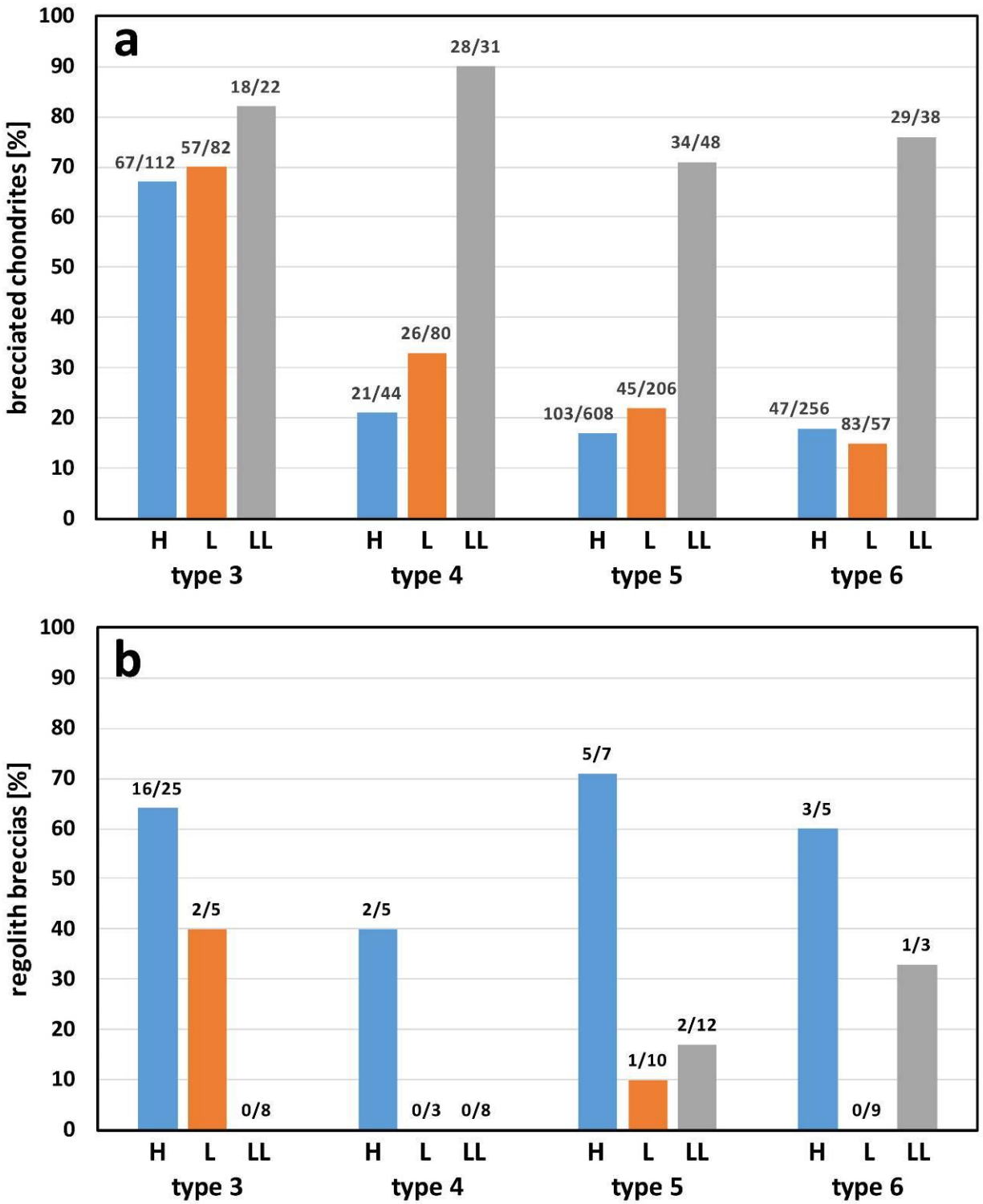
a
brecciated chondrites [%]
100
90
80
70
60
50
40
30
20
10
0
67/112
57/82
18/22
21/44
26/80
28/31
103/608
45/206
34/48
47/256
83/57
29/38
H
L
LL
type 3
type 4
type 5
type 6
b
regolith breccias [%]
16/25
2/5
0/8
2/5
0/3
0/8
5/7
1/10
2/12
3/5
0/9
1/3

Fig. 3

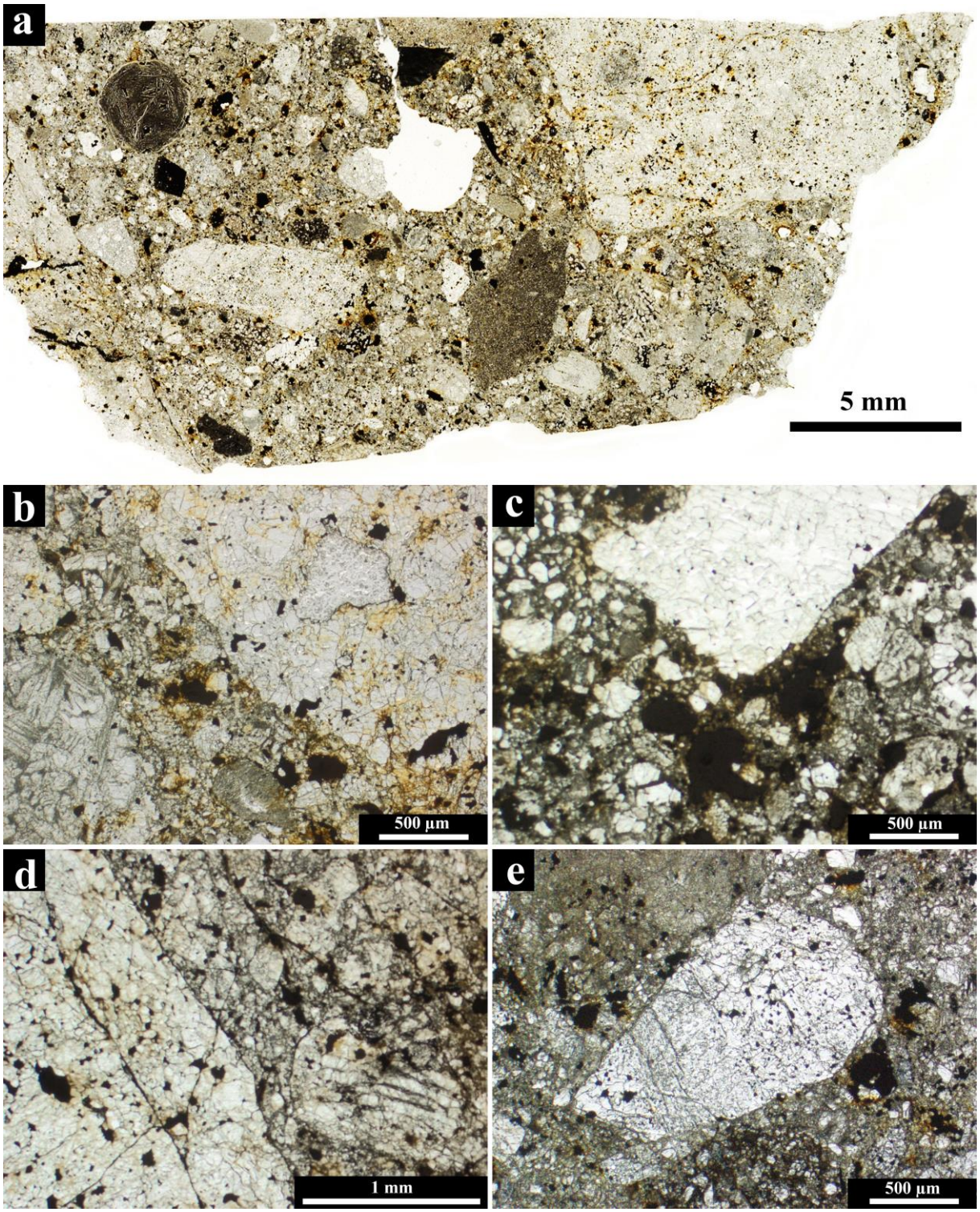


Fig. 4

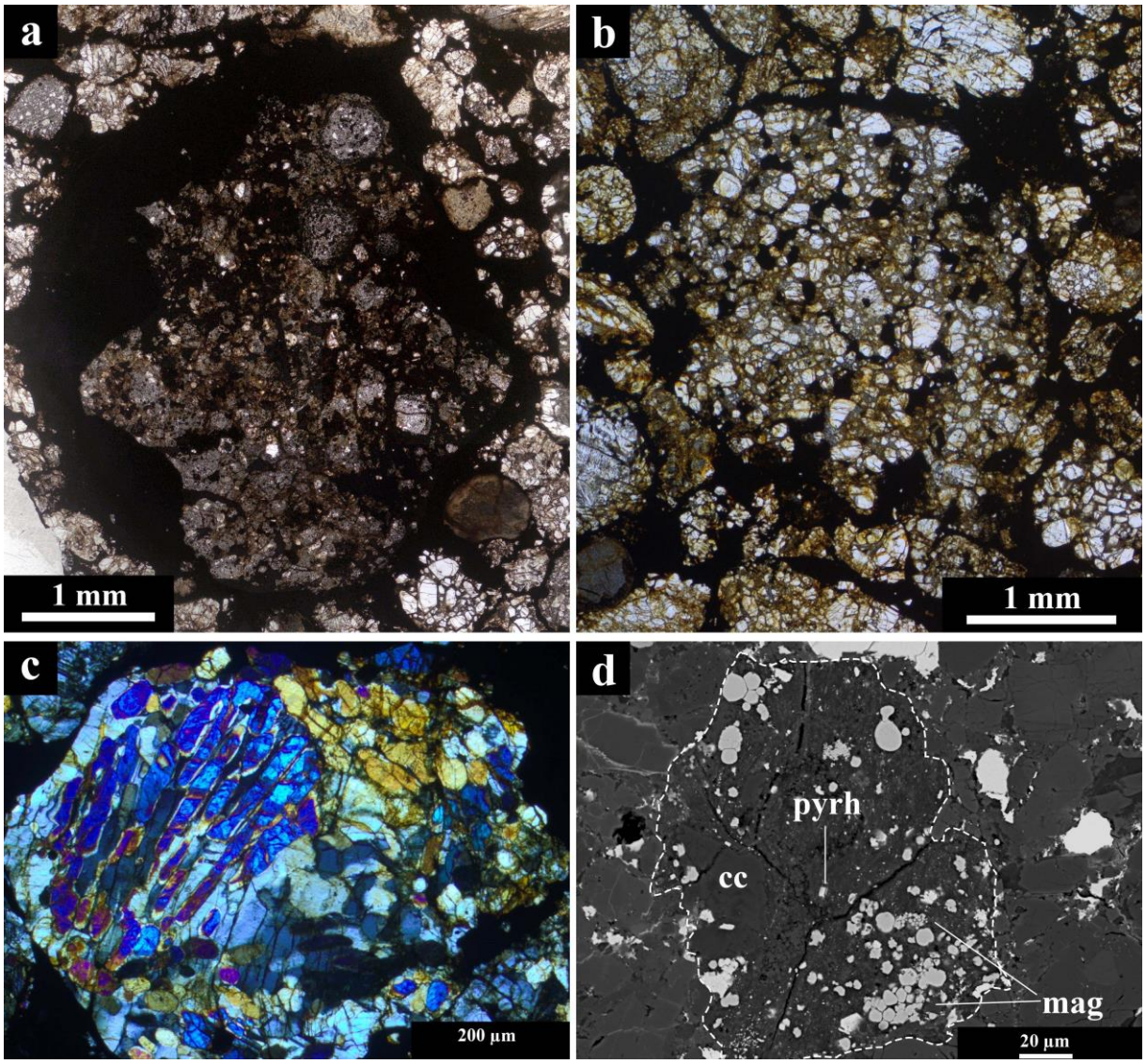


Fig. 5

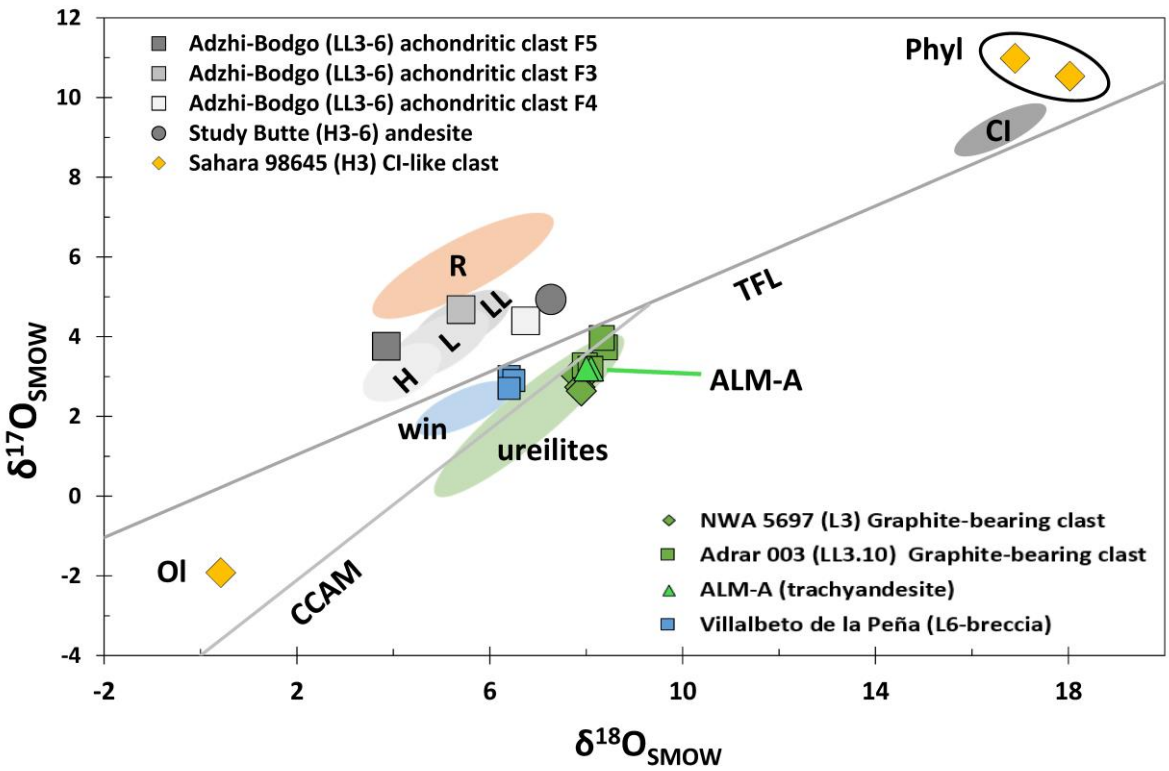
Adzhi-Bodgo (LL3-6) achondritic clast F5
Adzhi-Bodgo (LL3-6) achondritic clast F3
Adzhi-Bodgo (LL3-6) achondritic clast F4
Study Butte (H3-6) andesite
Sahara 98645 (H3) CI-like clast
Phyl
CI
R
LL
L
H
TFL
ALM-A
win
ureilites
Ol
CCAM
NWA 5697 (L3) Graphite-bearing clast
Adrar 003 (LL3.10) Graphite-bearing clast
ALM-A (trachyandesite)
Villalbeto de la Peña (L6-breccia)
δ17OSMOW
δ18OSMOW
12
10
8
6
4
2
0
-2
-4
-2
2
6
10
14
18

Fig. 6

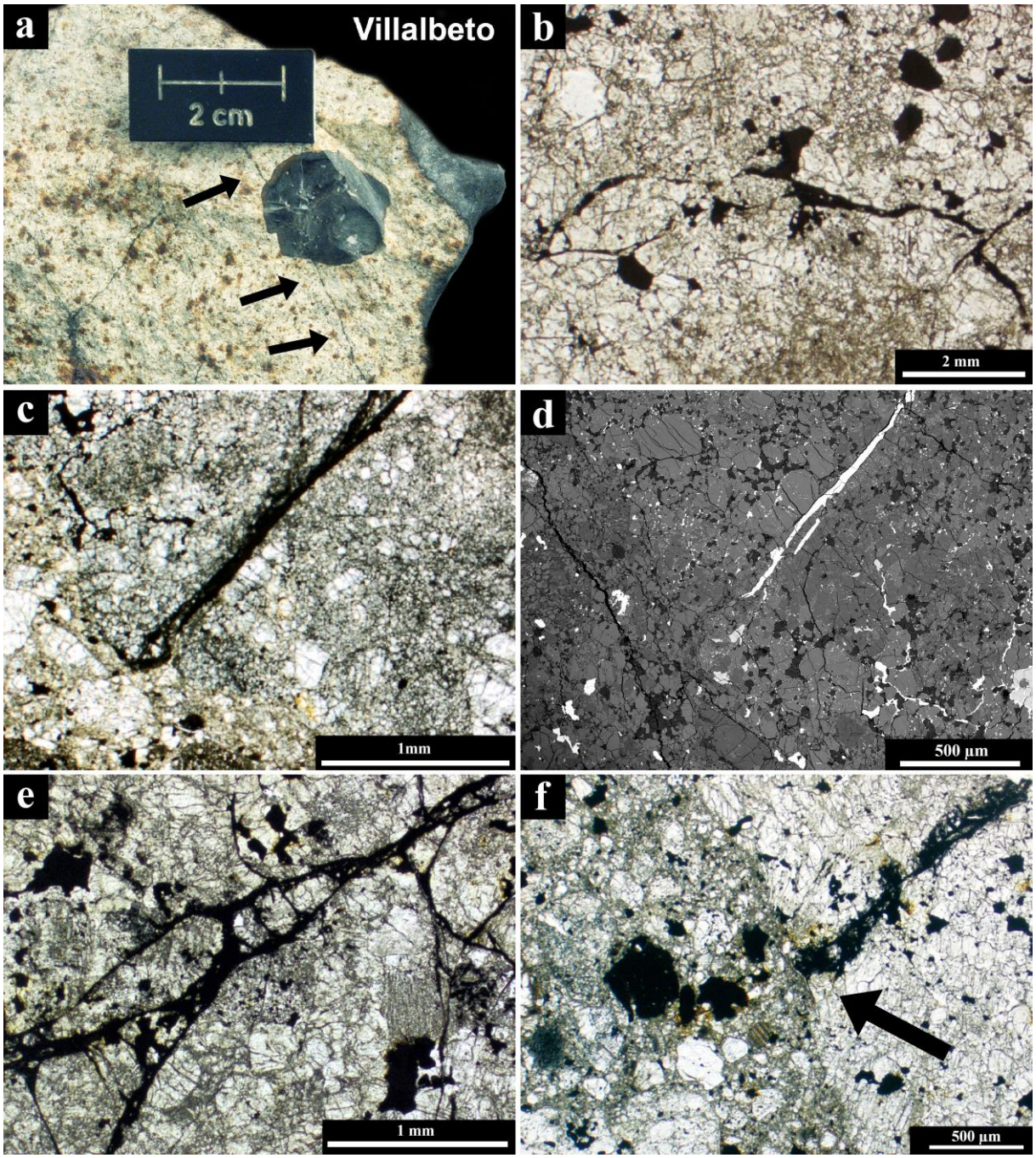


Fig. 7

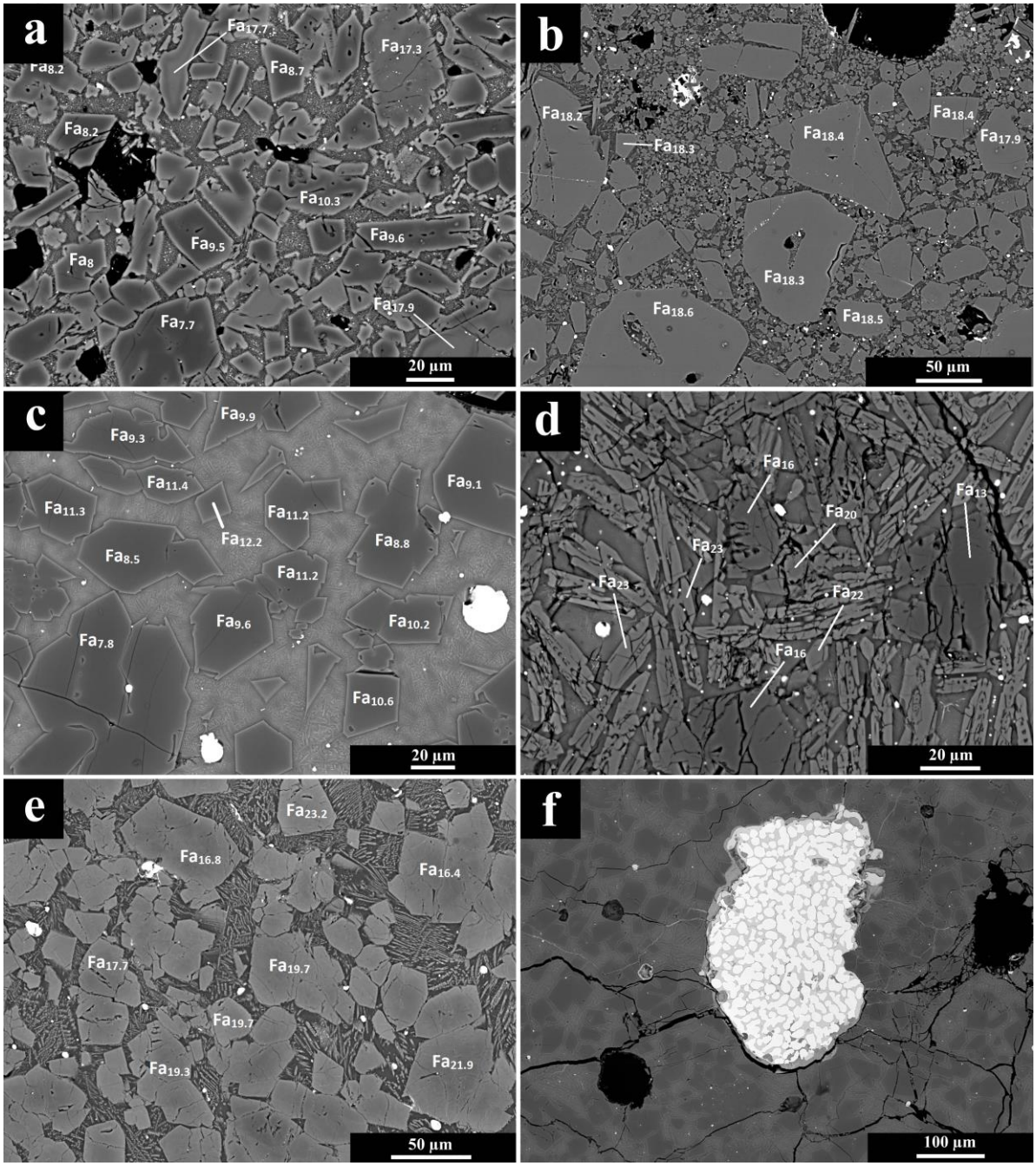
a
Fa17.7
Fa8.2
Fa8.7
Fa17.3
Fa8.2
Fa10.3
Fa9.5
Fa9.6
Fa8
Fa7.7
Fa17.9
20 µm
b
Fa18.2
Fa18.3
Fa18.4
Fa18.4
Fa17.9
Fa18.3
Fa18.6
Fa18.5
50 µm
c
Fa9.9
Fa9.3
Fa11.4
Fa9.1
Fa11.3
Fa11.2
Fa12.2
Fa8.8
Fa8.5
Fa11.2
Fa9.6
Fa10.2
Fa7.8
Fa10.6
20 µm
d
Fa16
Fa13
Fa20
Fa23
Fa23
Fa22
Fa16
20 µm
e
Fa23.2
Fa16.8
Fa16.4
Fa17.7
Fa19.7
Fa19.7
Fa19.3
Fa21.9
50 µm
f
100 µm

Fig. 8